Master's Thesis

Structure transformation of carbon nanotubes (CNTs) by heat treatment

Byungcheon Yoo

Department of Materials Science and Engineering

Graduate School of UNIST

2020

Structure transformation of carbon nanotubes (CNTs) by heat treatment

Byungcheon Yoo

Department of Materials Science and Engineering

Graduate School of UNIST

Structure transformation of carbon nanotubes (CNTs) by heat treatment

A thesis/dissertation
submitted to the Graduate School of UNIST
in partial fulfillment of the
requirements for the degree of
Master of Science

Byungcheon Yoo

06. 15. 2020 of submission
Approved by

_____

Advisor
Feng Ding

Structure transformation of carbon nanotubes (CNTs) by heat treatment

Byungcheon Yoo

This certifies that the thesis/dissertation of Byungcheon Yoo is approved.

06/15/2020 of submission

signature

_____

Advisor: Feng Ding

signature

_____

Zonghoon Lee: Thesis Committee Member #1

signature

_____

Han Gi Chae: Thesis Committee Member #2

signature

Abstract

Carbon nanotubes (CNTs) have been powerful candidates about various applications such as electronics, energy storages, composites for decades because their outstanding electrical, mechanical and structural properties. These properties heavily related to their structural features represented by chirality, diameter and number of walls. Therefore, structure controllable CNTs synthesis is indispensable for commercial applications. Despite of dedicated researches about effective synthesis method or post-treatment, still can't define precise mechanisms for homogeneity CNTs growth.

In this study, we tried heat treatment of single-walled carbon nanotubes (SWCNTs) and multi-walled carbon nanotubes (MWCNTs) as post-treatment method from 1700 ℃ to 3000 ℃ for 10 min by employing a rapid heating system which is based on joule heating that can heat up higher than 3000℃ quickly and characterized by Raman spectroscopy and transmission electron microscopy (TEM). We observed diameter enlargement of SWCNTs with increasing the temperature and MWCNTs specially, odd number of walls appear at higher than 2500 ℃. This result confirms mechanisms about transformation of SWCNTs to MWCNTs by SWCNTs bundle coalescence different from SWCNTs coalescence which induces enlarged diameter. The result of MWCNTs shows the quality improvement by defects healing and purifications at the temperature 3000 ℃ for 30 min.

Both experimental results demonstrate the effect of heat treatment as post treatment and can motivate to mechanisms for structure controllable CNTs

Contents

List of Figures

List of Tables

I. Introduction

1.1 Carbon based materials

Nanomaterials, especially, carbon-based multi-dimensional materials such as fullerene (0-D), carbon nanotube (1-D), graphene (2-D) and diamond (3-D) are carbon allotrope materials and have outstanding properties as mechanical, electrical, thermal, optical and etc. Due to these, carbon-based materials have been candidates in various fields including nanoelectronics, composites, bio-sensing and energy storage.

In 1985, H. W. Kroto *et al.*[1] discovered fullerene with consisting 60 carbon atoms called "Buckminsterfullerene" by laser irradiation (They won the Novel Prize for chemistry in 1996). This molecule consists of 12 pentagons and 20 hexagons with the shape like a spherical soccer ball (Fig. 1.1). The C_{60} is the smallest fullerene and each carbon atoms are sp^2 hybridized with all pentagons which are isolated by hexagons. There are two bond length, 6-5 junction and 6-6 junction. 6-6 junction is considered double bonds which cause restricting double bond in pentagon rings and easily react with electron rich type[2,3]

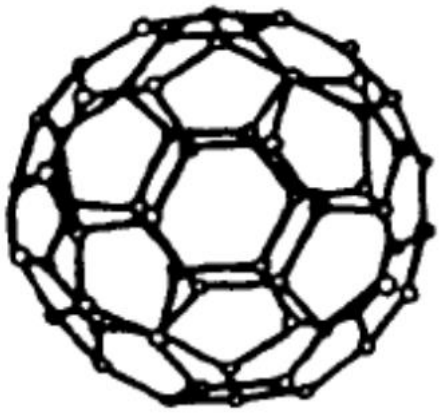

Figure 1.1 C_{60} Buckminsterfullerene (From Ref. [3])

In 1991, Sumio Iijima[4] found another novel material while doing produce fullerene with arc-discharge system, hollow tubular structure called "Carbon Nanotubes". The first observation of tube was multi-walled carbon nanotubes (MWCNTs) and after single-walled carbon nanotubes (SWCNTs) with diameters about 1 nm were found using metal catalysts in arc-discharge method[5] (Fig. 1.2). Carbon nanotubes also have sp^2 hybridized carbon atoms that each atom covalent bonded with 3 neighbor atoms

and considered as one-dimensional carbon allotrope because they have long length compared to the diameter; high aspect ratio. CNTs, simple-looking but outstanding properties affect by tube structure have attracted the attentions of many researchers how synthesize the CNTs with constant structure. This is because in order to apply to various fields, control the properties that are sensitive to structure is essential.

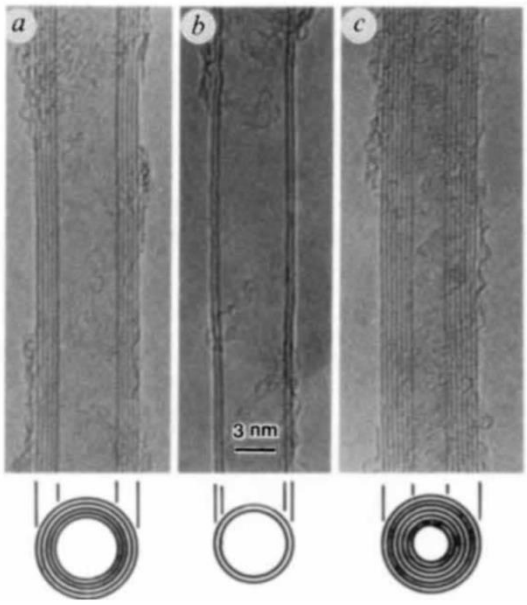

Figure 1.2 Electron micrographs of first observed carbon nanotubes (From Ref. [4])

2-dimensional carbon allotrope called "Graphene" is hexagonal honeycomb structure sp^2 hybridized material seems like one layer of graphite (Fig. 1.3). Because of atomic scale thickness, it has outstanding properties that high young modulus, strength, thermal, electrical conductivity and even transparent. In 2004, K. S. Novoselov *et al.*[6] introduced about tearing the single layer of graphite method using scotch tape (Andre Geim and Konstantin Novoselov won the Novel Prize for physics in 2010). Since then, extensive researches for single crystalline and large-scale synthesis methods that can make graphene more valuable material for various applications have been doing[7].

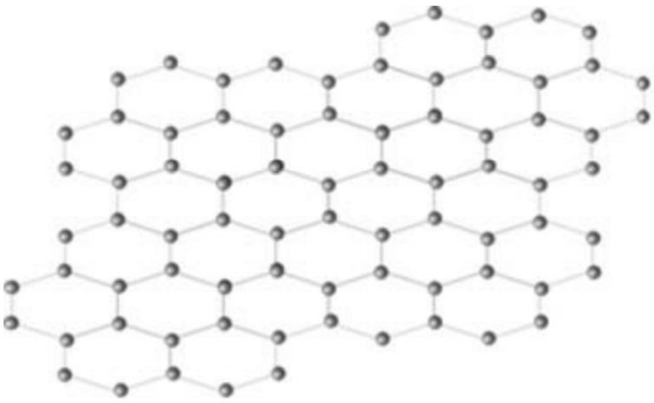

Figure 1.3 Graphene structure of a 2-dimensional hexagonal single sheet of carbon atoms (from Ref. [7])

Diamond is well known as the hardest material in the earth and low electrical conductivity because it has perfect sp^3 crystal structure with strong covalent bonds which is the clear difference between sp^2 hexagonal graphite structure; sp^2 is related to electrical properties and sp^3 is related to mechanical properties (Fig. 1.4)[8,9]. Diamonds are used in cutting, coating, and even in jewelry due to its remarkable properties on the other hand, graphite widely used in electrodes or heating elements.

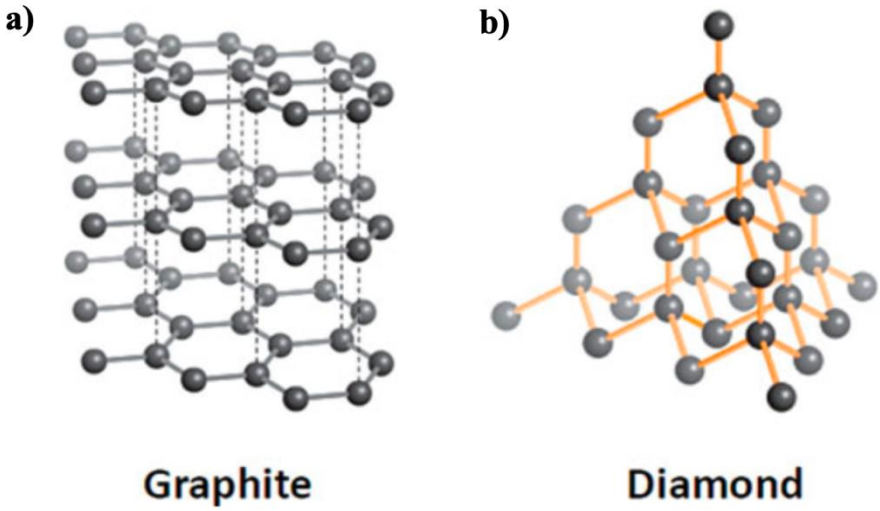

Figure 1.4 Crystal structure of (a) graphite (b) diamond (from Ref. [8])

1.2 Carbon nanotube (CNT)

1.2.1 Structure and properties of carbon nanotube (CNT)

Carbon nanotubes can be simply classified with the number of tubes as Single-walled carbon nanotubes (SWCNTs), Double-walled carbon nanotubes (DWCNTs), Multi-walled carbon nanotubes (MWCNTs) (Fig. 1.5). Single-walled carbon nanotubes shape like a rolled-up single-layer graphene sheet with diameter almost less than 2nm and multi-walled carbon nanotubes have multi-layers with broader diameter ranges. In multi-walled carbon nanotubes (MWCNTs), wall-wall distance is generally 0.34 nm that the same with the distance of each graphene layers in graphite[10]. There are two structural models in MWCNTs, one is Russian Doll model that consists separated nanotube for each wall and the other is Parchment model which forms wrapped around single graphene layer[11]. Table 1.1 shows the difference between SWCNTs and MWCNTs.

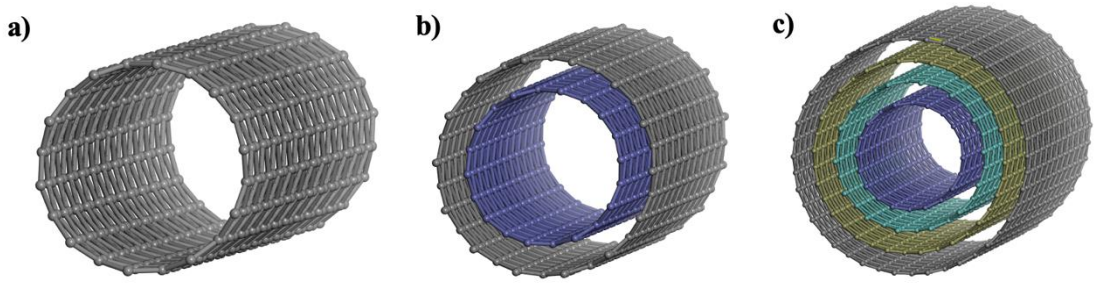

Figure 1.5 Classification of CNTs (a) Single-walled carbon nanotubes (b) Double-walled carbon nanotubes (c) Multi-walled carbon nanotubes

Table 1.1 Comparison between SWNT and MWNT (from Ref. [11])

SWNT	MWNT
Single layer of graphene	Multiple layers of graphene
Catalyst is required for synthesis	Can be produced without catalyst
Bulk synthesis is difficult as it requires proper control over growth and atmospheric condition	Bulk synthesis is easy
Purity is poor	Purity is high
A chance of defect is more during functionalization	A chance of defect is less but once occurred it is difficult to improve
Less accumulation in the body	More accumulation in the body
Characterization and evaluation is easy	It has very complex structure
It can be easily twisted and is more pliable	It cannot be easily twisted

The structure of carbon nanotubes is based on hexagonal honeycomb sp^2 carbon atom lattice that same with graphene sheet. Which direction the sheet rolled-up determines type of CNTs with chirality. It is specified with chiral vector (C_h), chiral index (n, m) and chiral angle (θ) (Fig. 1.6-7).

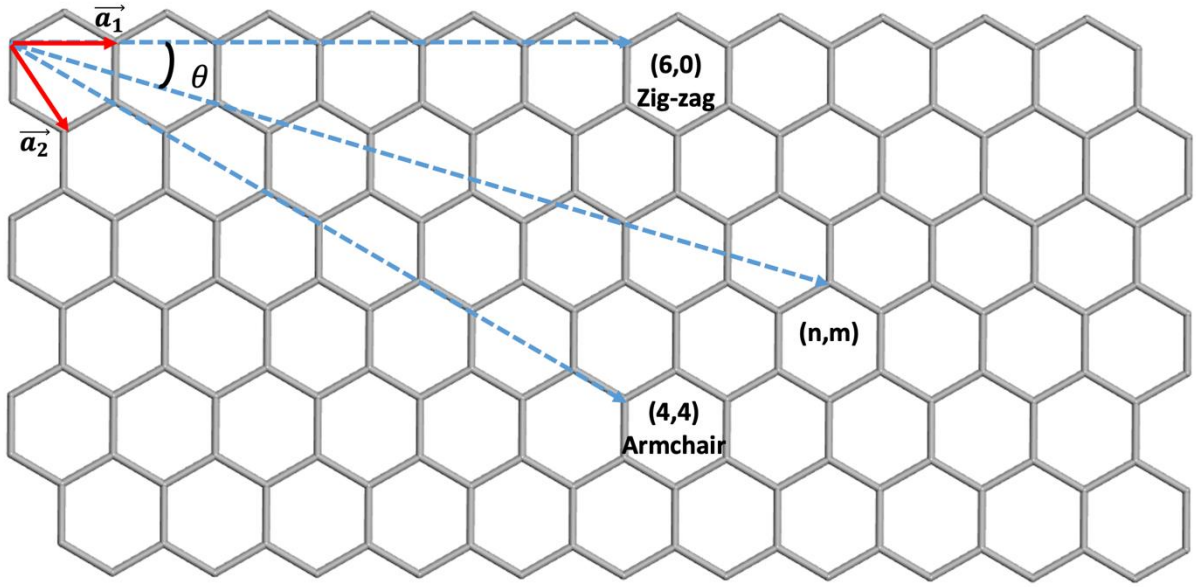

Figure 1.6 Hexagonal honeycomb graphene lattice showing specified CNTs structure

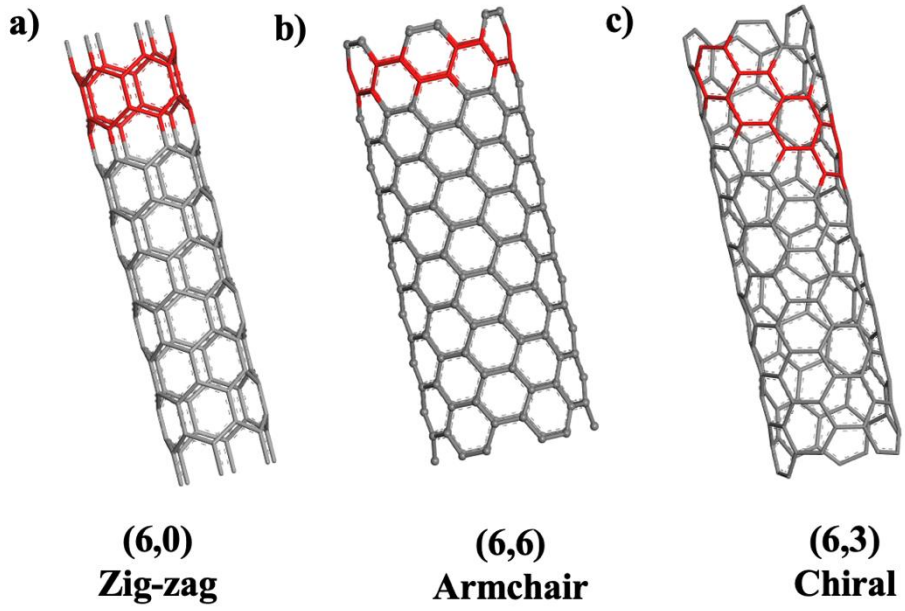

Figure 1.7 Different types of single-walled carbon nanotubes with different chirality (a) (6,0) zig-zag (b) (6,0) armchair (c) (6,3) chiral

The vector ($\overrightarrow{a_1}$, $\overrightarrow{a_2}$) is basic vectors in graphene lattice and (n, m) is integer which specify the defined chiral vector, $C_h = na_1 + ma_2$. This chiral vector forms chiral angle (θ) which ranges between 0° and 30° where chiral angle is 0°, that called zig-zag and angle with 30°, it is armchair direction[12]. The chiral angle in CNTs has important meaning because it not only determines the morphological structure, but also involves in electrical structure which band gap with metallic or semiconducting[13]. If the chiral index (n, m) has $n - m = 3k$, the SWCNTs are semi-metallic with small band gap or not, the SWCNTs are semiconducting with broader band gap[12]. Hence, SWCNTs can be applied to various applications through band gap adjustment with chiral homogeneity that is the most attractive point for next generation material and essential part that requires advanced study as well.

The CNTs have mechanical properties that very light weight but high tensile strength and elastic modulus from sp^2 covalent bonds among the carbon atoms. In 2000, M. F. Yu *et al.*[14] measured tensile strength of MWCNTs from 11 to 63 GPa. High aspect ratio with a hollow tube structure cause twist, kink and buckle when compressed in axial direction, but can restore its structure within limits[11,15]. Thermal conductivity of SWCNTs is about 2000 W/m K and MWCNTs of 3000 W/m K[16,17]. These properties show the possibility to replace metals for various fields.

Table 1.2 Comparison of Mechanical Properties of CNTs and Other Materials (From Ref. [15])

Comparison of Mechanical Properties			
Material	**Young's Modulus (TPa)**	**Tensile Strength (GPa)**	**Elongation at Break (%)**
SWCNT	~1 (from 1 to 5)	13-53[E]	16
Armchair SWCNT	0.94[T]	126.2[T]	23.1
Zigzag SWCNT	0.94[T]	94.5[T]	15.6-17.5
Chiral SWCNT	0.92		
MWCNT	0.8-0.9[E]	150	
Stainless Steel	~0.2	~0.65-1	15-50
Kevlar	~0.15	~3.5	~2
Kevlar[T]	0.25	29.6	

[E]Experimental observation ; [T]Theoretical prediction

1.2.2 Synthesis of carbon nanotubes

Since the discovery of CNTs with arc-discharge method[4], there have been designed to synthesis process for CNTs. The most popular synthesis methods are arc-discharge[4,18–20], laser ablation[21–24], Chemical Vapor Deposition (CVD) process[25–29]. Arc-discharge method is known as to produce high crystalline CNTs and schematic of this method is shown in Fig. 1.8. It consists of two graphite electrodes in vacuum chamber, especially anode is covered with carbon precursor and catalyst. When the D.C arc-discharge current is connected, it raises the temperature and carbon vapor which is evaporated from anode is deposited to opposite cathode. This process depends on some parameters such as gas condition, temperature, type of catalysts. Zujin Shi *et al*.[20] achieved the high yield SWCNTs using Y-Ni alloy as anode catalyst.

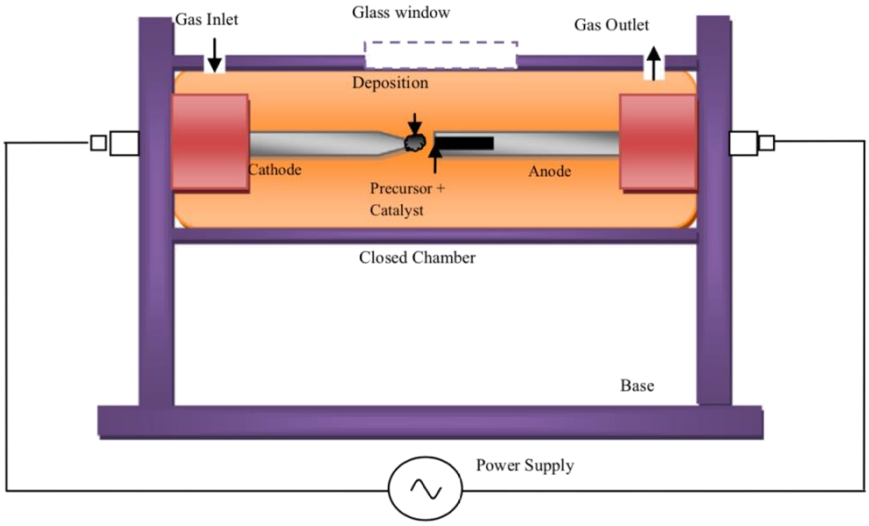

Figure 1.8 Schematic of arc-discharge method process (From Ref. [18])

Laser ablation method was first developed by Guo *et al*. in 1995[30] that known to much purer CNTs can be produced than arc-discharge[22]. Nd:YAG laser pulse evaporates the graphite target by high temperature in argon gas atmosphere and vapor phase carbon moves water-cooled copper collector along the argon flows direction[23,31] (Fig. 1.9). In this process, SWCNTs can be produced by adding transition metallic catalyst such as Ni-Co whereas MWCNTs from pure graphite[24].

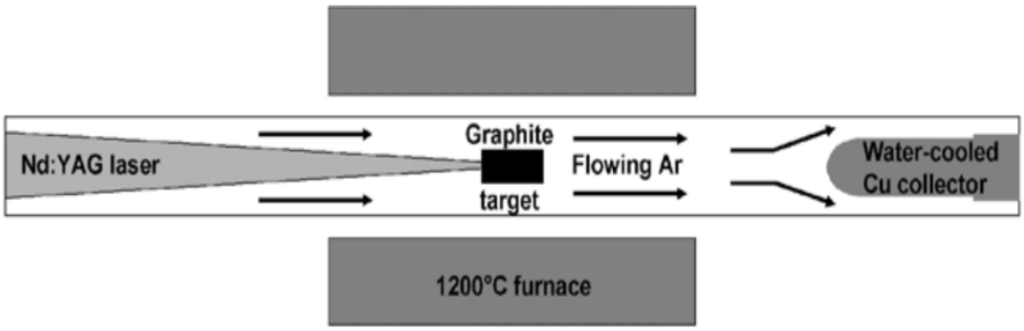

Figure 1.9 Schematic of laser ablation method (From Ref. [23])

Chemical Vapor Deposition (CVD) method is the most widely used process to synthesize the CNTs so far due to low-cost and high yield compares with arc-discharge or laser ablation method. Also, CVD provides various synthesis ways that can easily change growth condition as thermal CVD, catalytic CVD and plasma enhanced (PE) CVD[32]. Fig. 1.10 shows the schematic of a simple CVD process. Catalyst deposited on to substrate is put in the tubular furnace which inert gas atmosphere and heat to high temperature. Hydrocarbon gas as carbon precursor flow to furnace and CNTs can grow at the catalyst particle with decomposed carbon vapor by temperature. In this process, there are several parameters what we can control such as catalyst, temperature, pressure, growth time and carbon precursor which is the major advantage of CVD method. For example, catalyst size difference affects CNTs dimeter and commonly, CVD in low temperature can yield MWCNTs whereas, higher temperature creates SWCNTs.

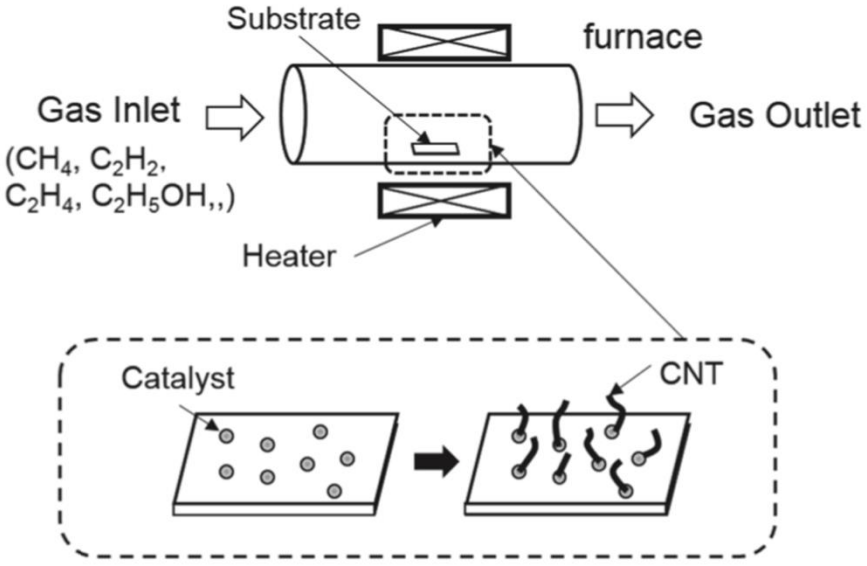

Figure 1.10 Schematic of simple CVD process (From Ref. [32])

Especially, P. Nikolaev *et al.*[29] designed the high pressure carbon monoxide (HiPCO) method that can produce with narrow diameter distribution (~ 0.7 – 1.2 nm) SWCNTs. This gas-phase method is synthesize SWCNTs by the decomposition of $Fe(CO)_5$ as catalyst in CO flowing as carbon precursor at high pressure atmosphere (Fig. 1.11)[28,29]. This process is proper to mass-production due to continuous catalyst and carbon feedstock gas flowing condition.

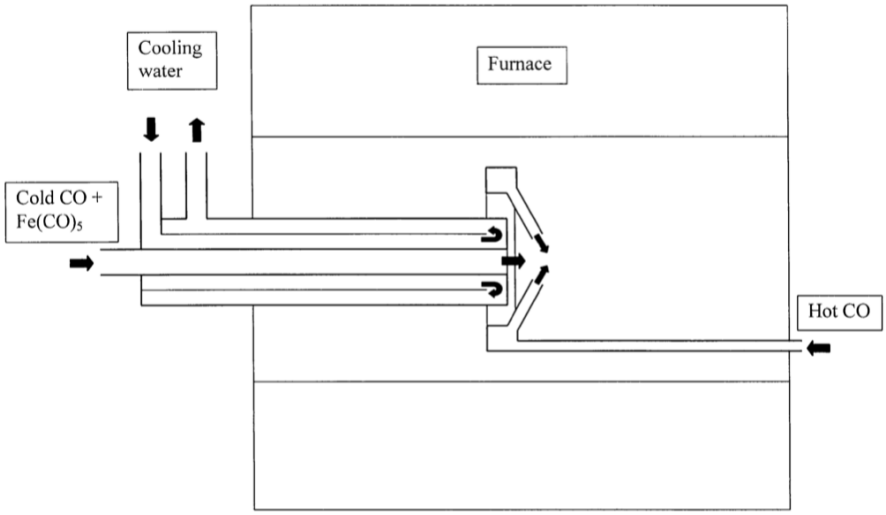

Figure 1.11 Schematic of high-pressure carbon monoxide (HiPCO) reactor (From Ref. [29])

1.2.3 Applications

Carbon nanotubes have been candidates for various potential applications about electrical nano devices, nanocomposites, energy storages and so on due to its advantages in outstanding properties. Firstly, CNTs are suitable for next generation electronics with their bandgap which is highly depend on diameter even flexible and transparent. S. Jang *et al.*[33] reported carbon based transistors which CNTs as a semiconducting channel and graphene as electrodes (Fig. 1.12a-b). These have excellent electrical performance due to negligible contact resistance between CNTs and graphene. Q. Cao *et al.*[34] introduced bendable and transparent thin-film transistors (TTFT) with SWCNTs networks (CNN) as all part of semiconducting and conducting layers on plastic substrate (Fig. 1.12c). Moreover, functionalized CNTs can be utilized for sensing device due to their sensitivity. M. He[35] report about CNTs sensor which is functionalized by cobalt(III) tetraphenylporphyrin for detecting N- nitrosamines (Fig. 1.12d).

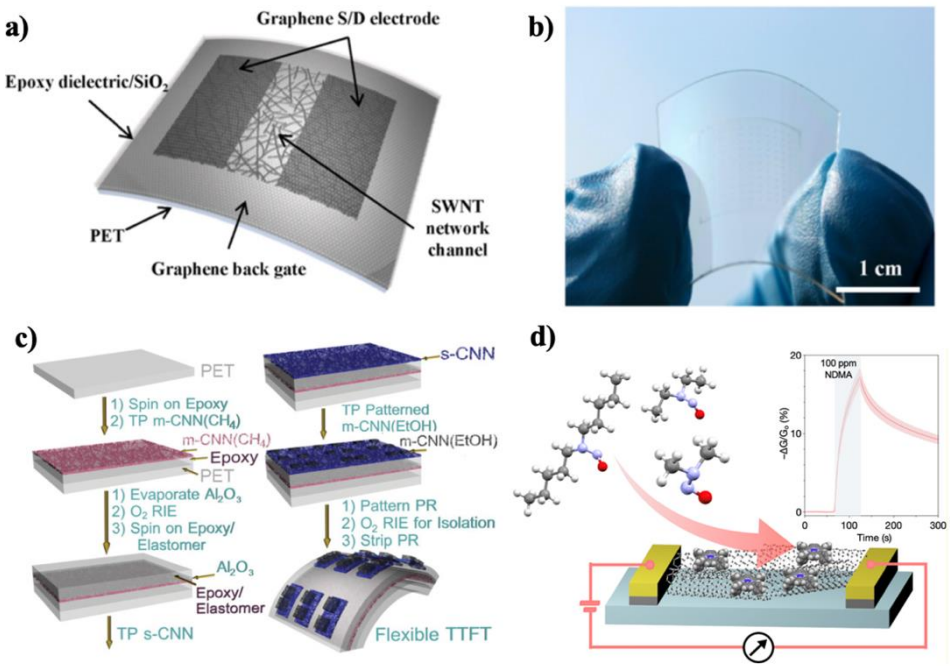

Figure 1.12 (a) Schematic of the carbon based flexible transparent thin film transistors (TTFTs) (From Ref. [33]) (b) Image of an optical transparent and bendable TFT device (From Ref. [33]) (c) Schematic illustration of the sequence of device fabrication procedures for CNN based flexible TTFTs (From Ref. [34]) (d) Schematics of CNTs sensors for *N*-Nitrosodialkylamines (From Ref. [35])

CNTs may most widely be used as composites with polymers that can enhance the mechanical strength or electrical, thermal conductivity[36]. Polyaniline-MWCNT nanocomposites applied for electromagnetic interference (EMI) shielding effect[37] and MWCNT-MnO_2/PPy as an anode in fuel

cells[38] improving electrical conductivity. In addition, CNT composites have been actively studied for aerospace industry called the forefront of material research because of its advantage of strong but light weight.

The hollow space size inside of CNT is determined by tube diameter that is controlled by synthesis process and this space is useful for energy storages or membranes[39–42]. R. S. Rajaura *et al.*[39] reported hydrogen storage capacity through functionalization of CNTs and introduced about storage sites of CNTs; i) inside the CNTs, ii) CNTs surface, iii) channel of CNTs, iv) grove of CNTs (Fig. 1.13a). S. Mi *et al.*[40] reported that the SWCNTs are much better than MWCNTs for hydrogen storages hence hydrogen capacity increases with SWCNTs size but, not in MWCNTs case. Fig. 1.13b shows the MWCNTs membrane which filter salt water and its permeability is also defined by entrance size of tube[42]

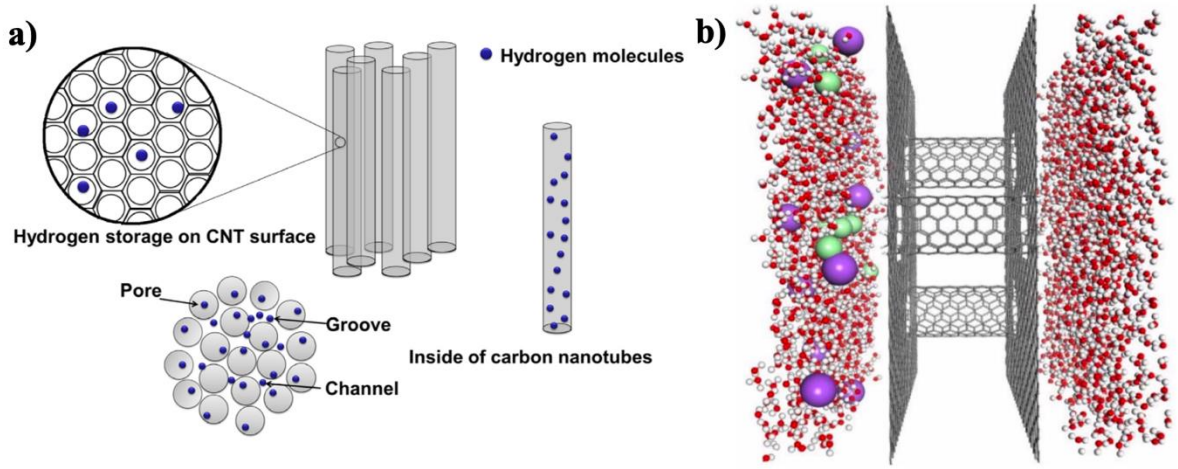

Figure 1.13 (a) Different storage sites of CNTs (From Ref. [39]) (b) Membrane with CNTs and graphene sheets for purifying Cl^- (green ions) and Na^+ (violet ions) in saltwater (From Ref. [42])

Beyond these applications, there are inexhaustible ways to utilize the outstanding properties of CNTs but, these are heavily influenced by its structural and topological features which highly affect the properties of CNTs. In this regard, many researchers have focused on growth mechanism of CNTs[26,43,44] and structure-controllable CNTs synthesis[25,27,45–48].

1.3 Previous literature

1.3.1 Heat treatment of CNTs

Unlike synthetic methods, heat treatment is well known to one of post-treatment methods. The growth mechanisms of CNTs are still not fully understood despite the many efforts of researchers. Therefore, post-treatment has been studied as to structural control of CNTs.

P. Nikolaev *et al*[49] introduced SWCNTs diameter doubling from coalescence of SWCNTs by heat treatment at 1400 ℃. They explained that the coalescence of SWCNTs is derived by reduced strain energy and same chirality can coalesce seamlessly. M. Yudasaka *et al.*[50] heat treated with HiPCO SWCNTs from 1000 ℃ to 2000 ℃ for 5 hour and expected that the diameter can increase by self-reconstruction because the results showed the diameters increased gradually but were not accorded with integer of pristine diameter. K. Méténier *et al*[51] experimentally demonstrated heat treatment of SWCNTs can cause the formation of MWCNTs at higher than 2200 ℃ and simulation works[52,53] supported these observations.

In 2002, M. Endo *et al.*[54] tried with DWCNTs from 1500 to 2400 ℃ and produced carbon bicable. They emphasized that the reconstruction by heat treatment can be utilized to control the structure and diameter and even creates distinctive carbon structure. R. Andrews *et al.*[55] introduced the effect of graphitization of MWCNT. They observed residual contents and microstructure defects are removed by high temperature heat treatment up to 3000℃. Priyanka H. *et al.*[56] also introduced the effect of heat treatment of MWCNTs by catalytic chemical vapor deposition (CCVD) method. As produced MWCNTs by CCVD method contain metal catalyst residues and have poor crystalline order, heat treatment can help to remove these and improvement the quality.

1.3.2 Coalescence mechanisms of CNTs

In 2000, M. Terrones *et al.*[52] introduced the “zipping” mechanism of coalescence of same chiral SWCNTs through theoretical simulation based on the results of electron irradiation to SWCNTs (Fig. 1.14). They mentioned that thermal process and sufficient available kinetic energy are needed to formation of interconnection. Besides, X. Yang *et al.*[57] introduced junctions between two non-orthogonal SWCNTs by heat welding.

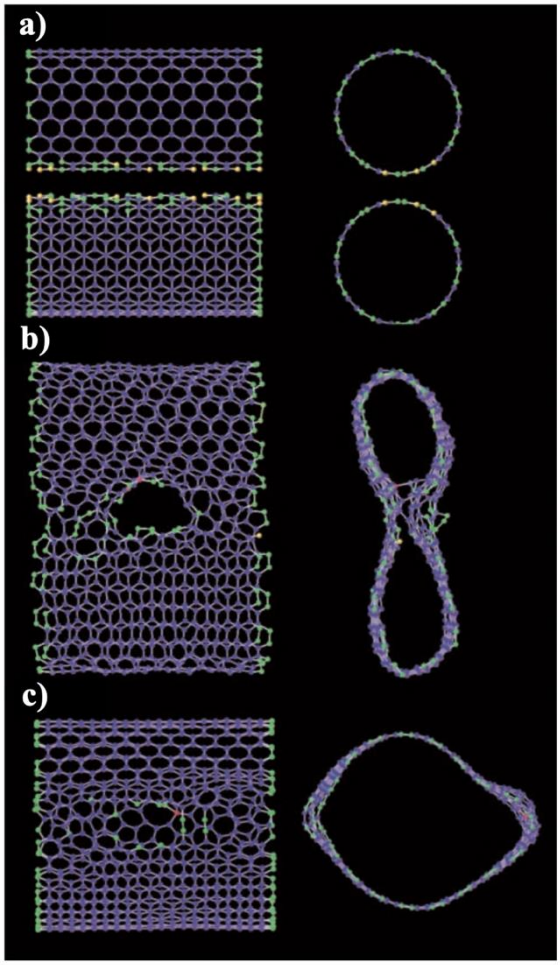

Figure 1.14 Coalescence between two parallel (10,10) carbon nanotubes into a larger diameter tube [side (left), cross section (right) (a) the creation of 20 vacancies in two adjacent nanotubes (b) The connected two carbon nanotubes with "zipping" mechanism (c) The coalesced larger tube about 2.6 nm (From Ref. [52])

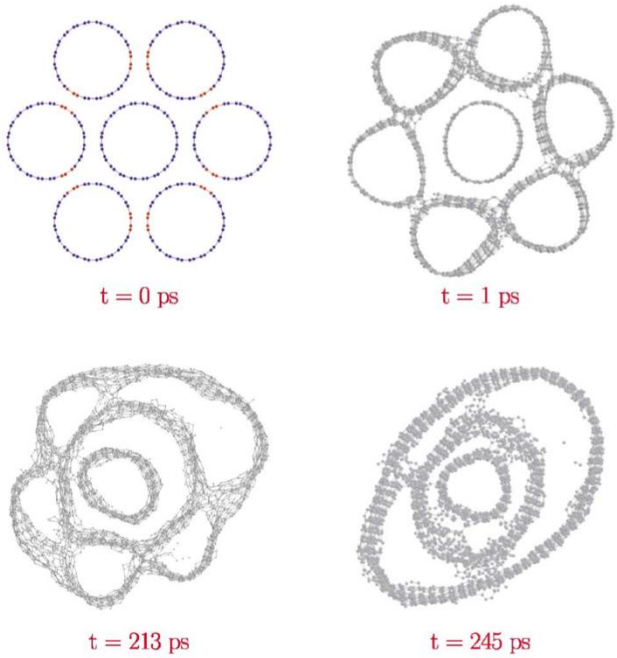

Figure 1.15 Snapshots showing the sequence of the transformation of seven single-walled carbon nanotubes bundle to multi-walled carbon nanotube (From Ref. [53])

M.J. López *et al.*[53] proposed a coalescence mechanism of SWCNTs bundle which surrounding around the center SWCNT. "patching and tearing" mechanism what they suggest can transform SWCNTs to MWCNTs (Fig. 1.15) and also they emphasized that thermal treatment higher than graphitization temperature (2200 ℃) is needed due to bundles of SWCNTs are thermal stable.

Inspired by these researches, we tried experimental study of heat treatment of HiPCO SWCNTs and MWCNTs from 1700 to 3000 ℃. Differ to previous process, we derived very short time (10 ~ 30 minutes) process by rapid joule heating system. Our results show that the diameter of SWCNTs increased with rising the temperature and SWCNTs transformed to MWCNTs from 2500 ℃ especially, most MWCNTs has odd number of walls such as 3- or 5-walled CNTs. We demonstrated the odd-even effect by coalescence of SWCNTs the support of previously proposed mechanism of transformation to MWCNTs. Also, we observed that several defects such as disconnected, bent and surface residues in the pristine MWCNTs disappeared and quality was improved by heat treatment at high temperature about 3000 ℃. These results were characterized with Raman spectra and Transmission Electron Microscopy (TEM) analysis.

II. Experimental details

2.1 Materials

HiPCO SWNT dry powder was purchased from ChemElectronics, Inc. Individual SWNT diameter is 0.8 – 1.2nm. MWNT powder was purchased from Sigma-Aldrich® produced by Catalytic Chemical Vapor Deposition (CCVD) method with 9.5nm average diameter. All of Specimens in this study were prepared in the graphite filament crucible made by carbon fiber without further purification. After treatment, the samples were dispersed in ethanol with Sodium Dodecyl Sulfate (SDS) for 1 hour by ultrasonication and they were analyzed with Raman spectra and transmission electron microscope (TEM).

2.2 Experimental methods

2.2.1 Rapid Heating System

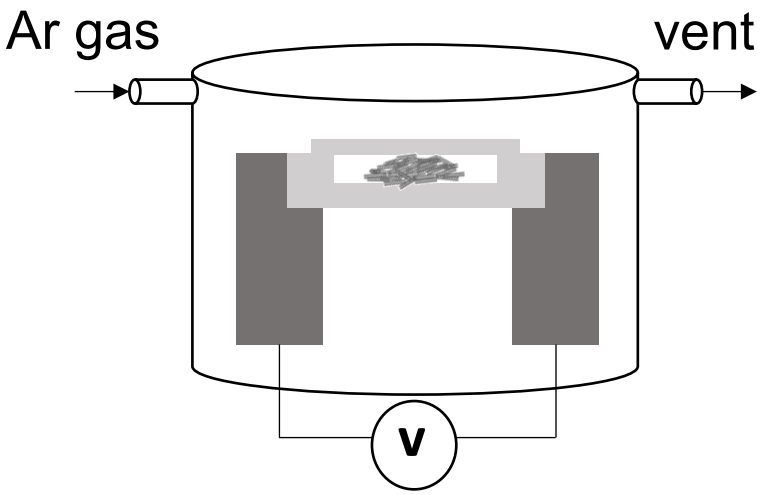

Figure 2.1 The schematics of Rapid heating system

Rapid heating system (Fig. 2.1) is designed by The IBS Center for Multidimensional Carbon Materials. Its operating principle is joule heating process with controlled by AC current up to 600 A and the temperature of graphite crucible was calibrated by pyrometer. Sample is enclosed inside of cap and graphite filament crucible which is connected with electrodes both sides. The heating elements, graphite crucible, converts electrical energy from electrodes into heat. Advantages of rapid heating system are very high ramping rate and users can control the working conditions such as pressure, gas condition

inside of chamber and even the ramping rate. In this study, with these features, ramping rate was set to 10 seconds and the pressure was 770 Torr with Ar flow condition. Both CNTs pristine samples were heat treated from 1700 ℃ to 3000 ℃ for 10 minutes and MWCNTs sample treated for 30 minutes additionally.

2.2.2 Raman Spectroscopy

Raman spectroscopy has been used for characterizing CNTs structure such as diameter, quality and electrical properties; semiconducting or metallic. Fig. 2.2. shows the atomic vibration types in CNTs. The Radial breathing mode (RBM) peak arises from 80 cm^{-1} to 300 cm^{-1} which caused by the vibrations of carbon atoms in radial direction[58] (Fig. 2.2a). Because it is peculiar mode that appears just in CNTs, it is most useful way to define the diameter of SWCNTs through the equation, $d = 248/\omega_{RBM}$[59,60].

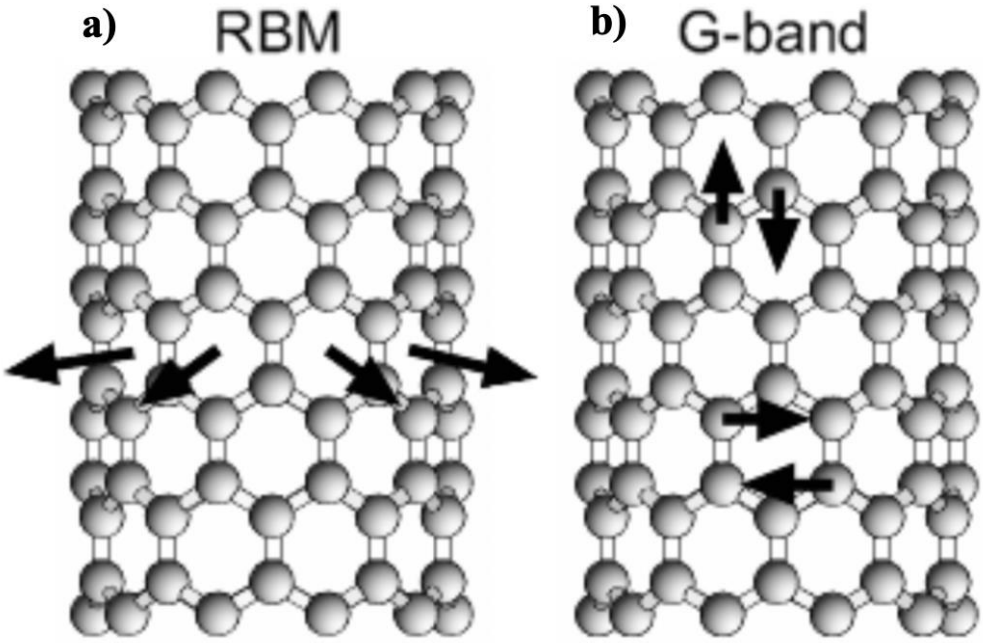

Figure 2.2 Schematics of the atomic vibrations for a) the RBM and b) the G band modes (From Ref. [58])

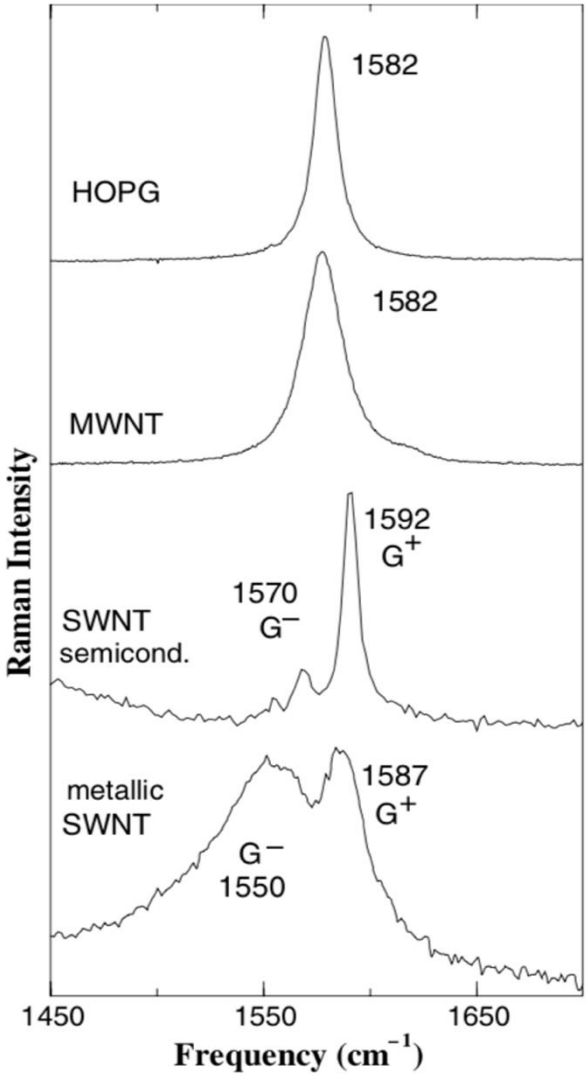

Figure 2.3 G band for highly ordered pyrolytic graphite (HOPG), MWNT bundles, semiconducting SWNT and metallic SWNT (From Ref. [58])

The G band which is called tangential mode seems like stretching of C-C bonding can be observed about 1580 cm^{-1} (Fig. 2.2b). It can show the electrical properties of tube which is semiconducting or metallic with two separate peaks, G^+ and G^- peak.

As shown in Fig. 2.3, there are different line shape of G peak among each tube characters. Compare with semiconducting SWNT, the Lorentzian line shape, the metallic SWNT has broaden G^- peak which is related to free electrons in CNTs[58,61]. In addition, G peak somewhat depends on the diameter of tube as MWNT which has large diameter outer tube appear single G peak that similar with graphite[60].

At last, D band around represents defects. As the intensity of the D peak increases, there are more defects so, G/D ratio has been mainly used to assess the quality of CNTs. Due to the MWNT is hard to

evaluate from RBM or G peak, G / D ratio is much used to estimate its structure.

In this study, we used Raman spectroscopy with 532 nm green laser to characterize the diameter and quality of CNTs.

2.2.3 Transmission Electron Microscope (TEM)

Transmission Electron Microscope (TEM) is the most powerful method to analyze the structure of CNTs such as the inner and outer walls diameter, number of walls, defects and chirality[62].

To take the TEM, we dispersed the sample powder into ethanol with Sodium Dodecyl Sulfate (SDS) as surfactant with ultrasonication for 1 hour and drop onto a copper grid. TEM images were used for determining the diameter, number of walls and figuring out the quality of CNTs.

III. Results and discussions

3.1 HiPCO SWCNTs

3.1.1 Pristine HiPCO SWCNTs

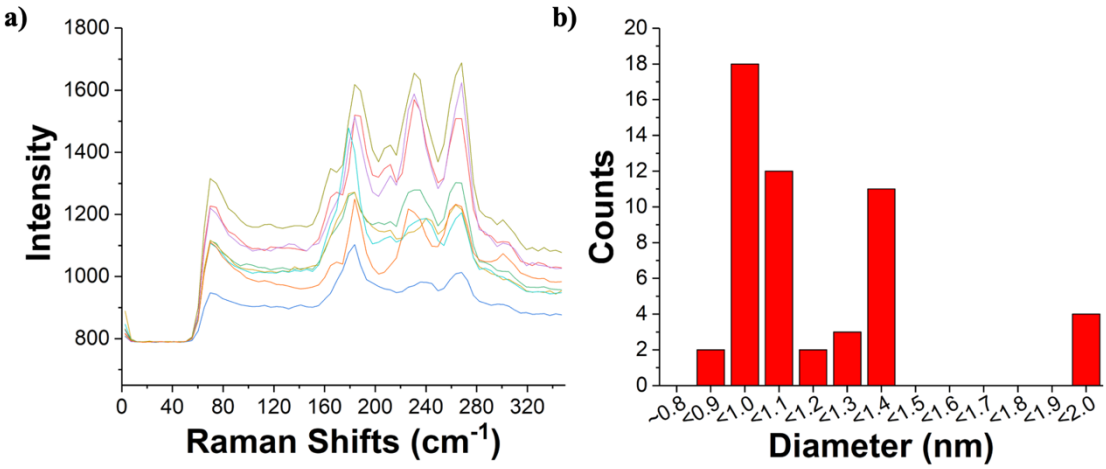

Figure 3.1 Characterization of pristine HiPCO SWCNTs (a) Raman RBM peaks (b) diameters distribution

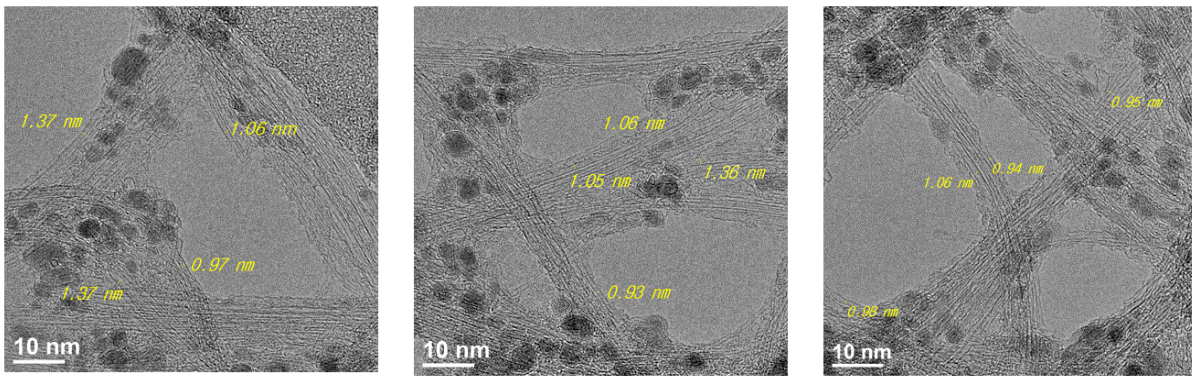

Figure 3.2 TEM images of pristine HiPCO SWCNTs

The diameters of pristine HiPCO SWCNTs were characterized with Raman RBM peaks and TEM images then identified the distribution of diameters (Fig 3.1-2). As shown in Fig. 3.1a, dominant RBM peaks of pristine sample emerge at 183, 231, 267 cm^{-1} which are correspond to diameters of 1.35, 1.07, 0.93 nm by using the equation of $d = 248/\omega_{RBM}$[59]. From TEM images (Fig. 3.2), we can observe they are the form of bundle structure containing many iron clusters and also figure out the most diameter have 0.9 ~ 1.3 nm.

3.1.2 Raman Spectroscopy

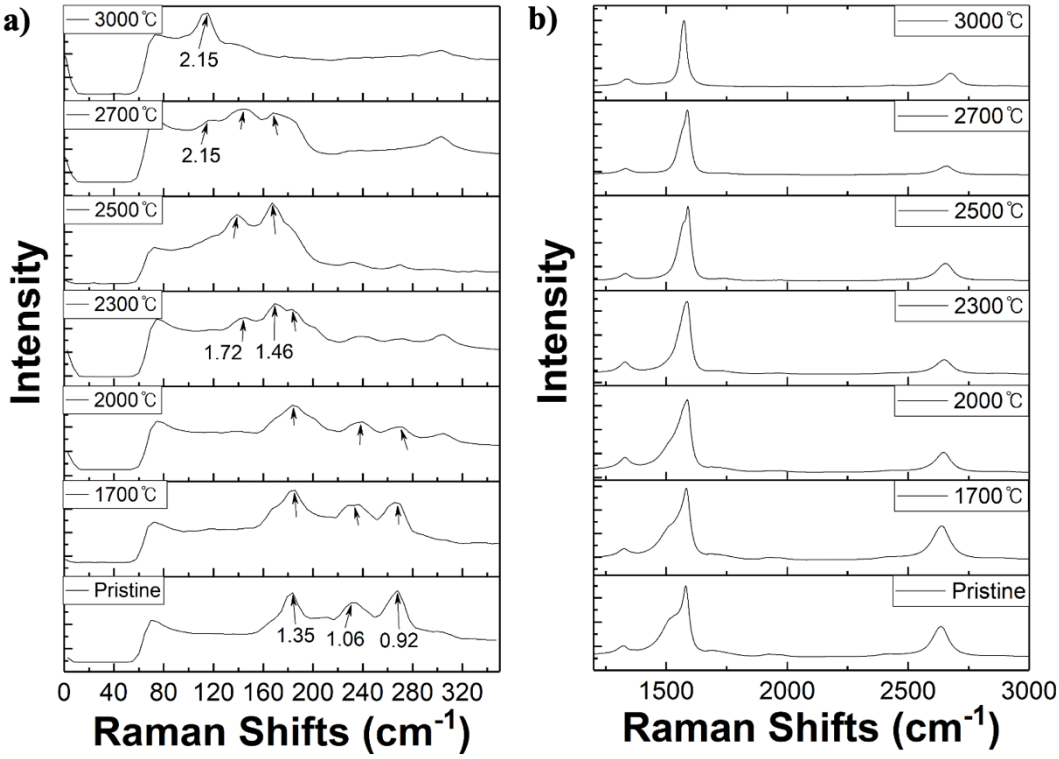

Figure 3.3 Raman spectra of heat-treated HiPCO SWCNTs at each temperature (a) Raman RBM peaks (Estimated diameters (nm) are indicated with arrow mark) (b) D, G, 2D peaks

Fig. 3.3a shows the RBM peaks which indicate diameter changes by heat treatment from 1700 to 3000 ℃ for 20 minutes. Under 2000 ℃, the pristine three RBM peaks (183, 231, 267 cm^{-1}) are still dominate but the ratio of high frequency ones (231, 267 cm^{-1}) keep decreasing that imply the smaller SWCNTs gradually enlarge. In this part, diameter around 2 nm doesn't appear in RBM peak. So, it is thought that enlarged SWCNTs under 2000 ℃ are caused by self-reconstruction, not a coalescence. From temperature at 2300 ℃, new RBM peak (144 cm^{-1}) which correspond with 1.72 nm emerge and it is close to the doubling of smallest pristine SWCNTs about 0.9 nm that considered coalescence with each other. When the heat treatment temperature was higher than 2700 ℃, 115 cm^{-1} peak (2.15 nm) which considered to coalescence of SWCNTs around 1.06 nm is appear. Although, it is hard to figure out the diameter larger than 2.5nm form RBM peak, there may has larger tubes and we think that the doubling of large SWCNTs requires much higher temperature than smaller ones.

Also, Fig. 3.3b shows the G peaks (1580 cm^{-1}) of SWCNTs. We can estimate that the left shoulder of G peak around 1550 cm^{-1} is gradually decreased with the temperature increasing and disappears.

This is explained to the disappear of small diameter and metallic SWCNTs which is less stable than the semiconducting SWCNTs[58,63].

From Raman results, we considered the HiPCO SWCNTs structure transformation mechanisms by heat treatment. Firstly, small diameter SWCNTs are enlarged more and more by the structural reconstruction and then start to coalescence at higher temperature.

3.1.3 Transmission Electron Microscope (TEM)

To support the results from Raman spectra (Fig. 3.3), heat treated HiPCO SWCNTs were characterized with the transmission electron microscopy (TEM) (Fig. 3.4-9). Though diameters of SWCNTs cannot show evident change until 2000 ℃, iron clusters in tubes were eliminated comparing with pristine SWCNTs images (Fig. 3.2). At 2300 ℃, also, tubes still remain as single-walled tube structure, but the diameters are significantly enlarged.

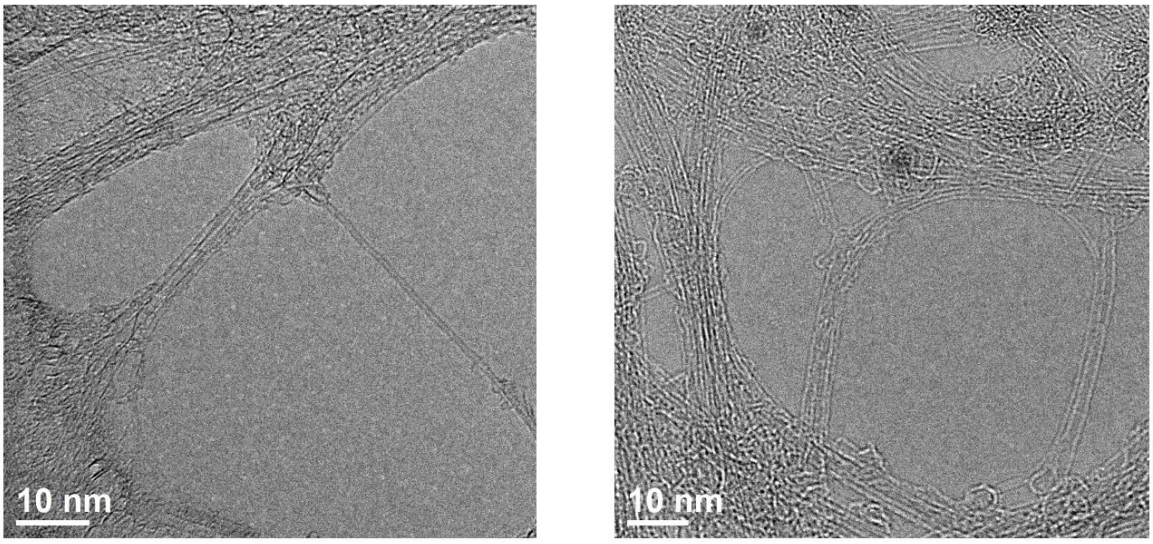

Figure 3.4 TEM images of heat treated HiPCO SWCNTs at 1700 ℃

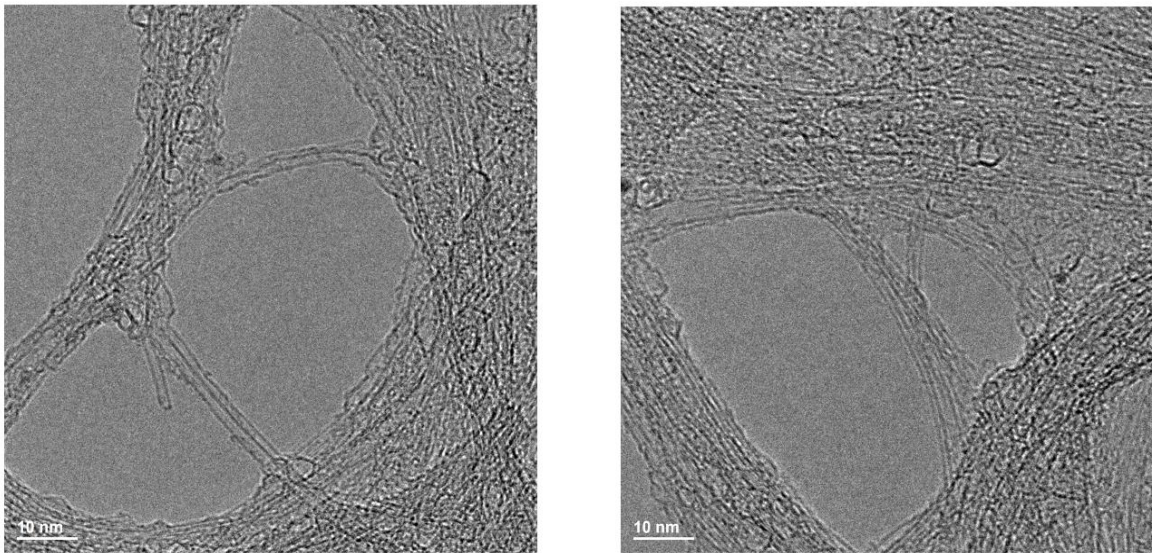

Figure 3.5 TEM images of heat treated HiPCO SWCNTs at 2000 ℃

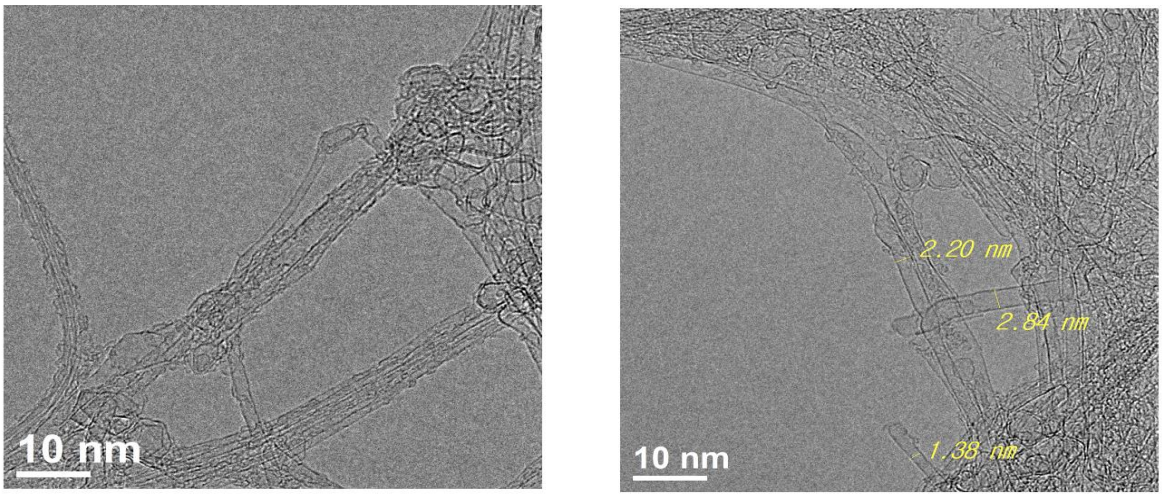

Figure 3.6 TEM images of heat treated HiPCO SWCNTs at 2300 ℃

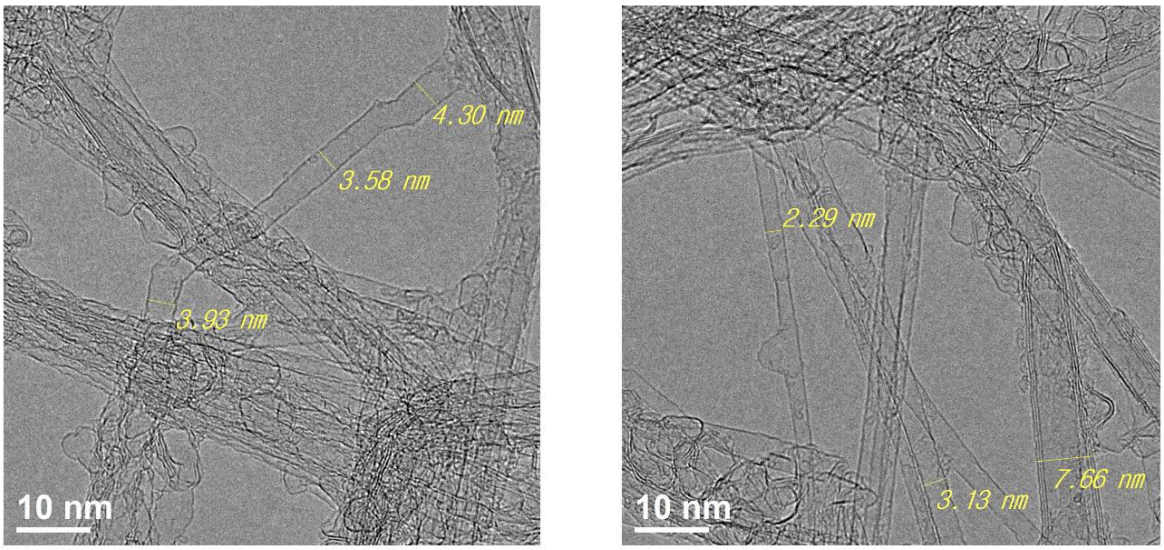

Figure 3.7 TEM images of heat treated HiPCO SWCNTs at 2500 ℃

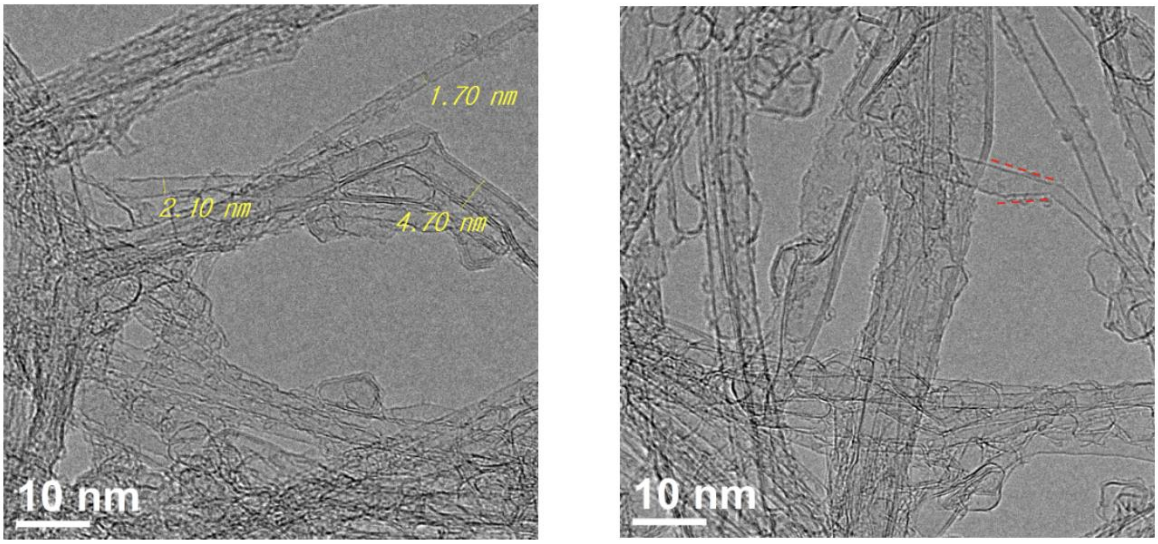

Figure 3.8 TEM images of heat treated HiPCO SWCNTs at 2700 ℃ (red dotted marks show unique structures)

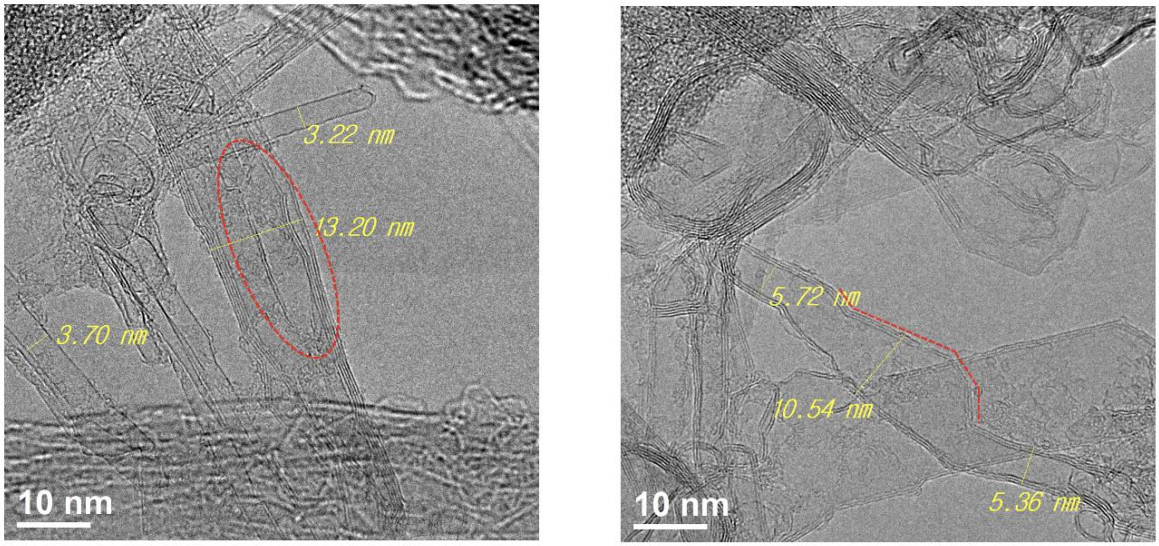

Figure 3.9 TEM images of heat treated HiPCO SWCNTs at 3000 ℃ (red dotted marks show unique structures)

From 2500 ℃ (Fig. 3.7), SWCNTs commence to transformation to MWCNTs and those are much larger than enlarged SWCNTs. MWCNTs emerge more and more with increasing temperature and the number of walls increased. Also, we can see that the number of tubes in each bundle are much smaller than the pristine bundles. These imply that the SWCNTs in bundles are coalesced by heat treatment. In addition, some unique features such as bent junction, irregular diameters in one tube and different gaps of each walls are occurred (red dotted marks in Fig 3.8-9).

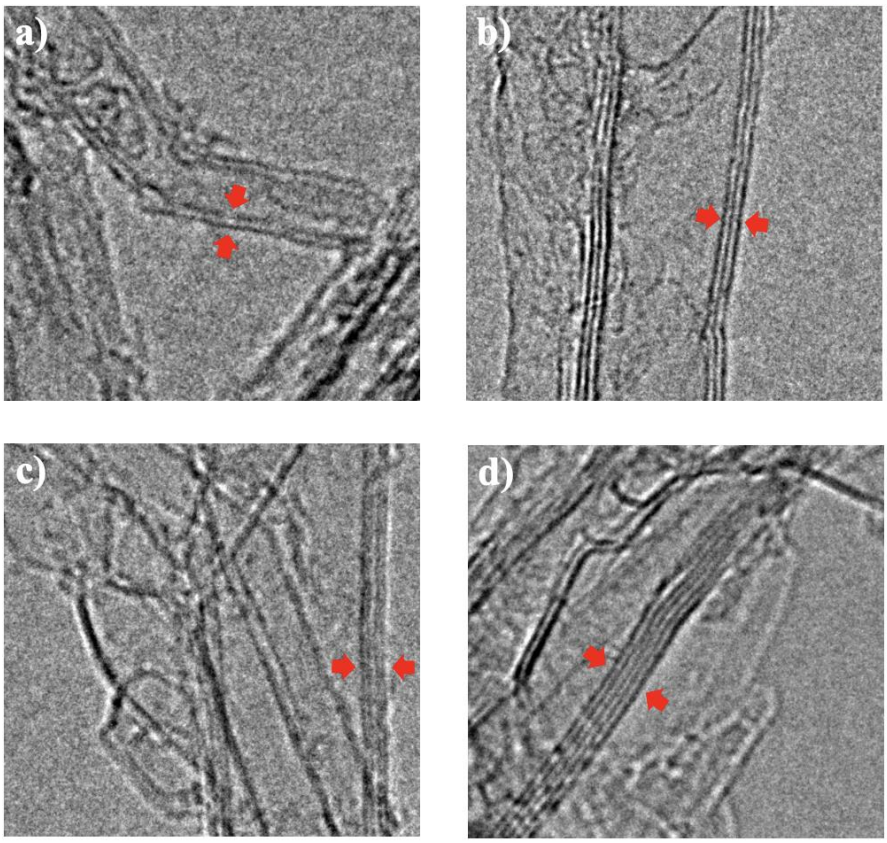

Figure 3.10 TEM images for each number of walled carbon nanotube after heat treatment at 2700 ℃ (a) double-wall (b) triple-wall (c) 4-wall (d) 5-wall

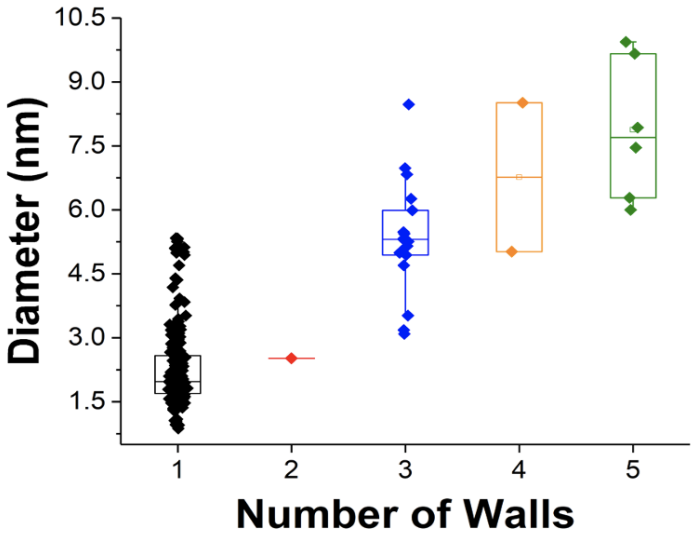

Figure 3.11 Statistics about diameter and number of tube walls after heat treatment at 2700 ℃

To further study, we characterized the number of walls in MWCNTs after heat treatment at 2700 ℃ (Fig. 3.10) and got the statistics based these TEM images (Fig. 3.11). We can figure out that the distribution of CNTs diameter range is much broader than pristine samples and all of smaller than 1 nm CNTs are disappeared which implies that the small diameter CNTs are coalesced with each other and transformed to larger ones.

Above all, the most unique feature is that the even number (double-, 4-walled tube) of CNTs are hard to find out comparing with odd number (triple-, 5-walled tube). Among the 180 CNTs samples, we just observed only one DWCNTs and two 4-walled CNTs but, 17 triple-walled and 6 5-walled CNTs (Fig. 3.11). This phenomenon makes possible to predict novel mechanism that the transformation of even number of CNTs is prohibited during the coalescence of SWCNT bundles.

3.1.4 Mechanisms about SWCNTs bundle transform to MWCNT

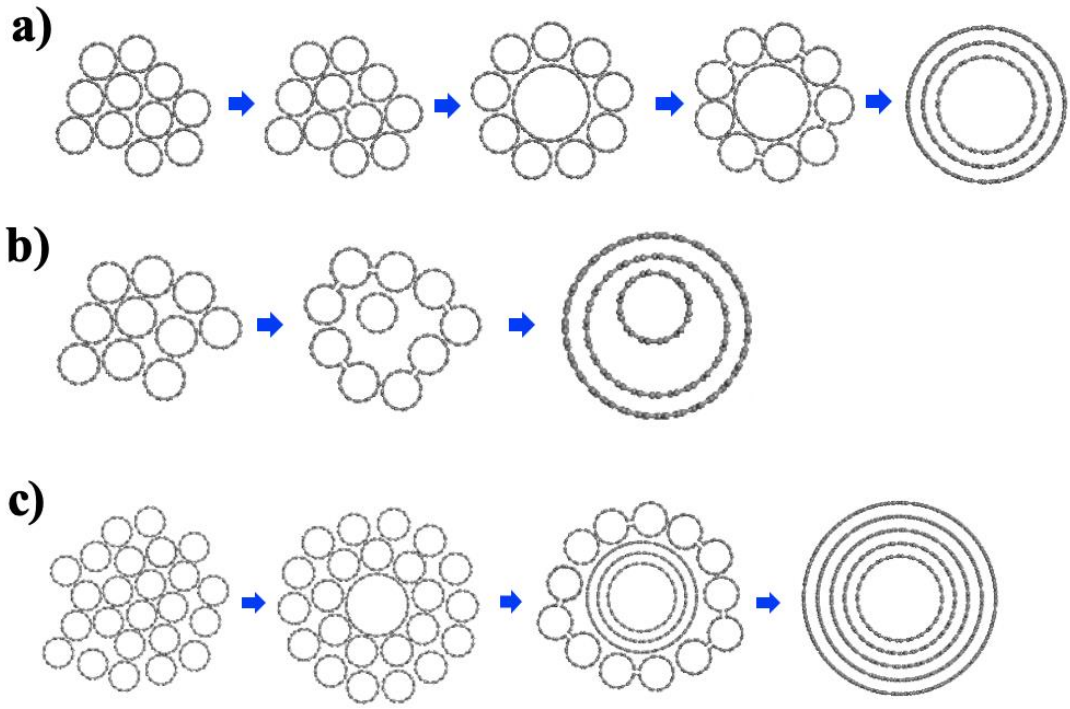

Figure 3.12 (a) Mechanism of transform to odd number of CNT (b) Mechanism of coalescence of different diameter in one tube (c) Mechanism of transform to 5-walled CNT in bundle with far more tubes

With these results, we expected two coalescence mechanism of SWCNTs bundles, one is triple-walled CNT with uniform wall-wall distance and the other is triple-walled CNT which has irregular wall-wall

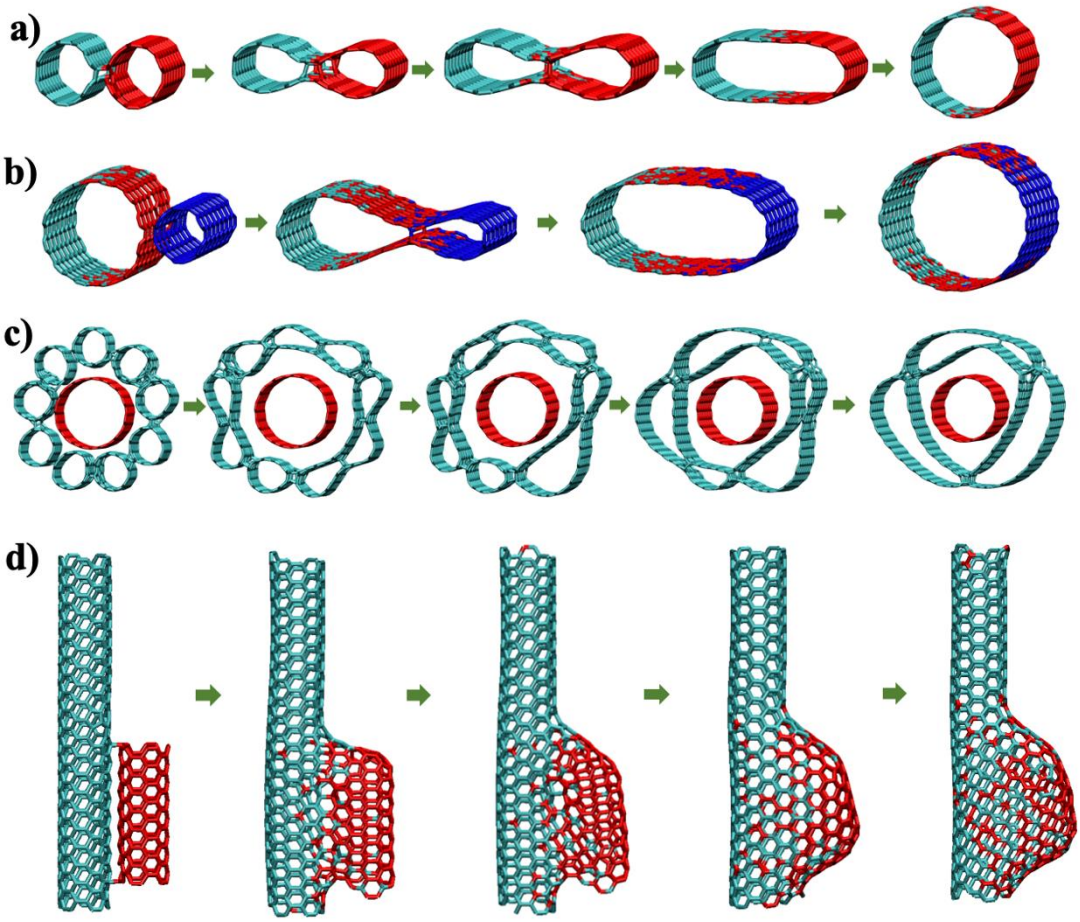

Figure 3.13 (a-b) The sequential coalescence of (6,6) SWCNTs (c) The spontaneous coalescence of nine (6,6) SWCNTs around (12,12) SWCNT (d) The coalescence of different length of (5,5) SWCNTs (Provided by Ziwei Xu in Prof. Feng Ding's group)

distance (Fig. 3.12a-b). Also, this process can be proceeded to the formation of 5-walled CNTs by applying much more SWCNTs around triple-walled CNT (Fig. 3.12c). EDKMC simulations were performed to support suggested mechanisms (Fig. 3.13). Fig. 3.13a-b show the sequential coalescence of (6,6) SWCNTs. Two (6,6) SWCNTs coalesce each other with junction firstly and the C-C bonds connecting the top and bottom carbon layers break gradually due to the decreasing of the high curvature energy of system in this part and finally, (12,12) SWCNT is formed[64–66]. Further coalescence with (6,6) SWCNT again, the tube is still SWCNT with enlarged diameter which means that the sequential coalescence of SWCNTs leads to just larger single-wall like SWCNT diameter doubling observed by P. Nikolaev *et al.*[49]. Distinct mechanism from that, explain the spontaneous coalescence of SWCNTs bundle (Fig. 3.13c). Surrounding (6,6) SWCNTs around (12,12) SWCNT merge together and junctions among them disappeared gradually as they coalesce. Eventually, this process leads to triple-walled CNT which also agrees with mechanism of MWCNT growth proposed by M.J. López *et al.*[53]. Also, Fig.

3.13d can explain unique structure observed in TEM images (Fig. 3.8-9 red dotted mark).

The main contents that can be derived from these results are as follows. The sequential coalescence of SWCNTs small bundle induce a large SWCNT and the spontaneous coalescence of surrounding SWCNTs always add two layers to center SWCNT. So, MWCNTs by coalescence of SWCNTs bundle has (2n+1) wall restricting the even number of walls.

3.2 MWCNTs

3.2.1 Raman Spectroscopy

MWCNTs are hard to analyze with RBM peaks due to its large diameter, feature characterization with Raman spectra is limited to G, D peaks. Pristine MWCNTs powder was heat treated from 2500 ℃ and 3000 ℃ for 10 min and further tried with 3000 ℃ for 30 min because there were no dramatic changes.

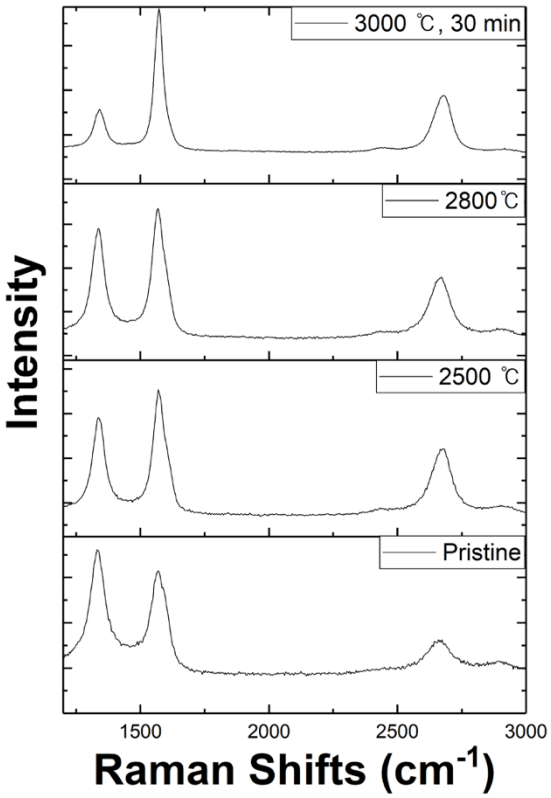

Figure 3.14 D, G, 2D peaks in Raman spectra of heat-treated MWCNTs at each temperature

Fig. 3.14 shows the D, G and 2D peaks of each MWCNTs samples. G/D ratio is most efficient way to evaluate defects in CNTs which the higher value means the better quality. In pristine sample, D peak has higher intensity than G peak with G/D ratio, 0.991. After heat treatment at the temperature 2500 and 2800 ℃, the intensity of G peaks is higher than D peaks of which G/D ratio ≈ 1, that still seems similar to pristine sample. When heat treated at 3000 ℃ for 30 min, the G/D ratio is increased almost 1.2 which indicates that the increase of crystalline region and improved purity. These results seem to be related to the previous research by W. Huang *et al.*[67] about heat treatment of MWCNTs as the efficient purification method, but they described that defect healing of MWCNTs takes a long time.

3.2.2 Transmission Electron Microscope (TEM)

To further study about the quality changes by heat treatment, we compared pristine sample and heat treated at 3000 ℃ for 10 min with TEM and high resolution TEM (HR-TEM). Fig. 3.15 shows TEM images of the pristine MWCNTs which have many defects such as rough surface, broken tube and amorphous carbon in inner tube. These defect types are specified by HR-TEM images (Fig. 3. 16).

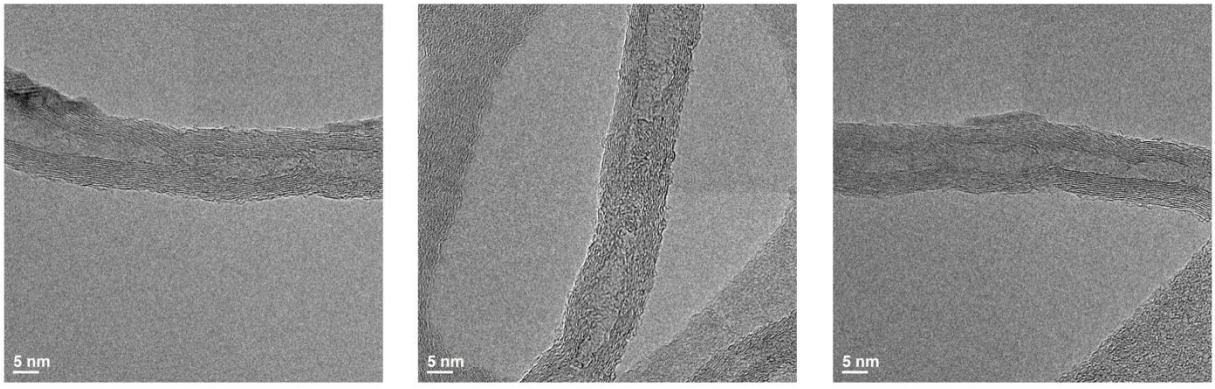

Figure 3.15 TEM images of pristine MWCNTs

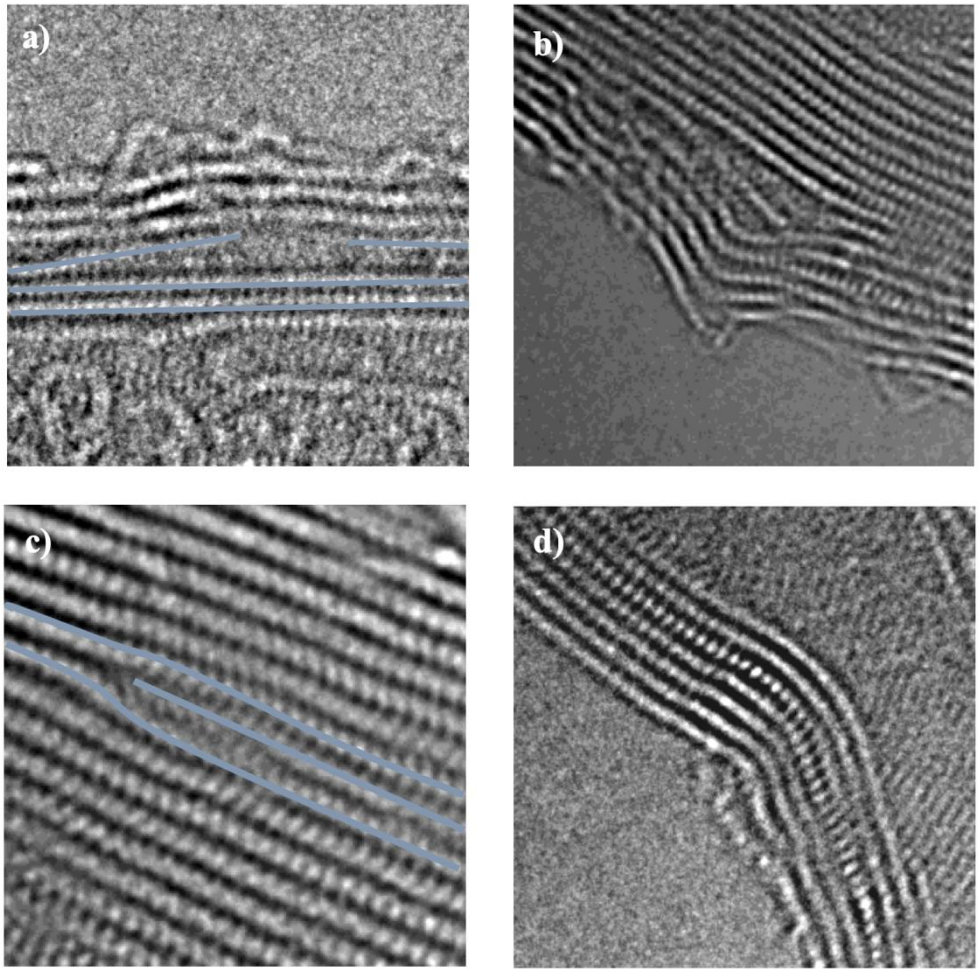

Figure 3.16 HR-TEM images of defect types in pristine MWCNTs (a) disconnection (b) buckling (c) edge dislocation (d) kink structure (Provided by Jongchan Yoon in Prof. Zonghoon Lee's group)

In comparison with pristine MWCNTs, improved MWCNTs after heat treatment are shown in Fig. 3.17-19. The most evident change between pristine and heat-treated samples is surface defects improvement. Besides rough and residual surface in pristine, heat-treated samples are smoother and much straight although residues were not completely removed (Fig. 3.18). Fig. 3.19 shows bamboo-like MWCNT of which growth process is known to the accumulation of carbon atoms at catalyst particle in particular, inner part of tube that is already growing and this atoms grown to graphitic sheet by forming joint with the wall[68–70]. Similar to this mechanism, disconnected amorphous graphitic region can grow new tube by connecting each other due to confined high concentrate carbon atom which is confined in outer tube.

Furthermore, this study has advanced research potential by characterizing the chirality of tubes with electron diffraction pattern from HR-TEM because what we expect is that various chirality of each walls in one tube will become monotonous by post-treatment.

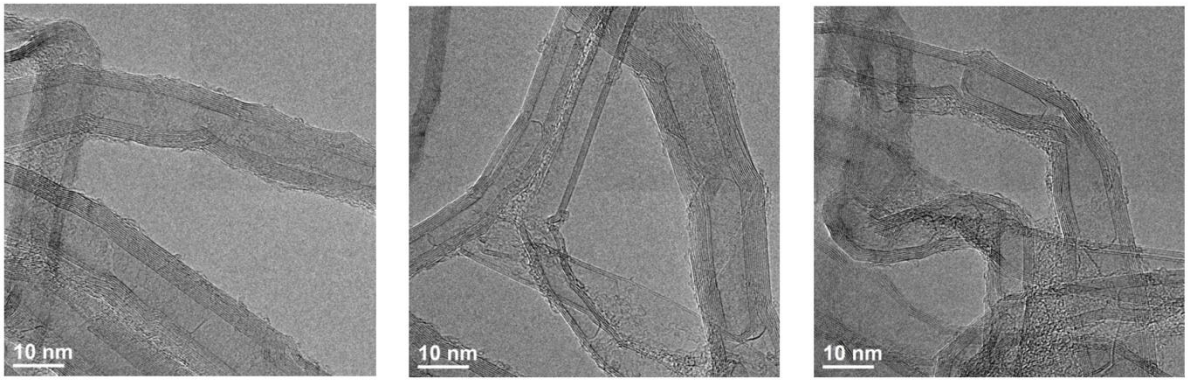

Figure 3.17 TEM images of heat treated 3000 ℃, 30 min MWCNTs

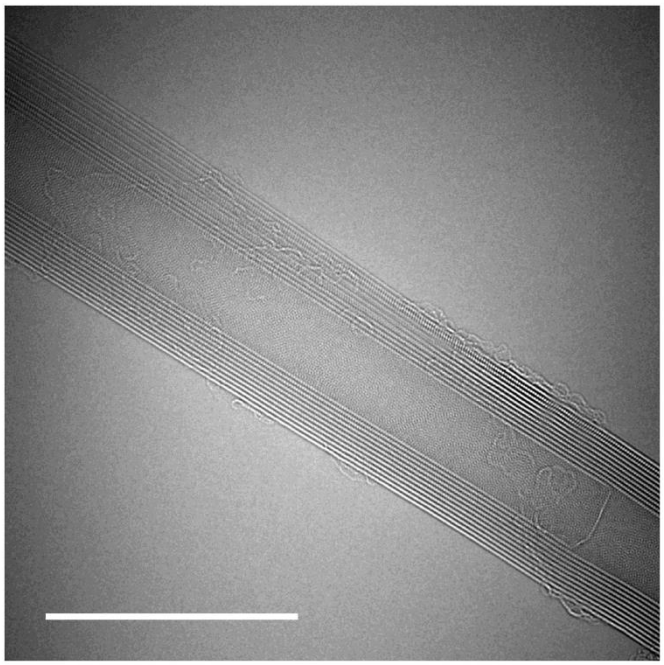

Figure 3.18 HR-TEM images of heat treated 3000 ℃, 30 min (provided by Jongchan Yoon in Prof. Zonghoon Lee's group)

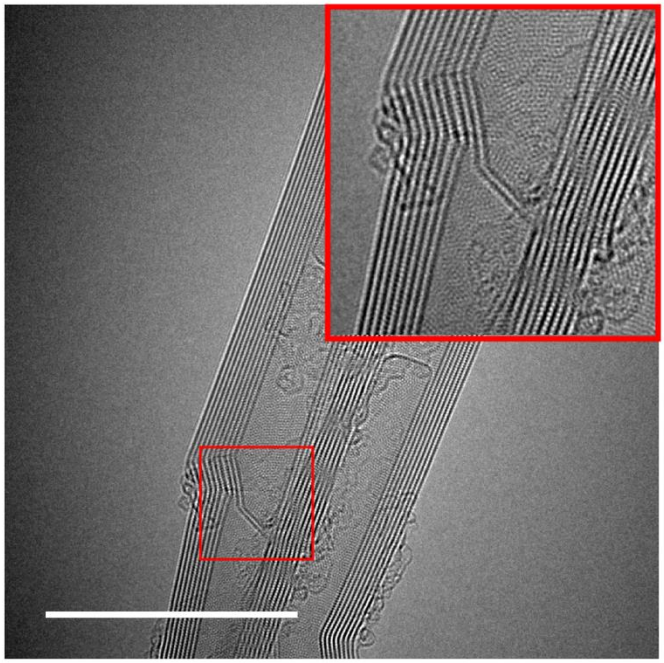

Figure 3.19 HR-TEM images of heat treated 3000 ℃, 30 min (bamboo structure in red square) (provided by Jongchan Yoon in Prof. Zonghoon Lee's group)

IV. Conclusions

We studied about the structure transformation of SWCNTs and MWCNTs by heat treatment.

Firstly, we observed that the diameter of SWCNTs gradually enlarged from 2000℃ but at higher than 2500℃, the small bundles coalesce to large diameter one and the large bundles lead to MWCNTs. Also, we found some unique nanostructures such as SWCNTs which have different diameter in one tube and irregular diameters MWCNTs. It is that SWCNTs are unstable at high temperature and the surrounding environment is a key factor that determines transformation structure like enlarged SWCNTs or MWCNTs especially odd number of walls. Through these results, we suggested the novel mechanism which SWCNTs transform to odd number of walls MWCNTs by heat treatment

Next is the study about structural change of MWCNTs during heat treatment. Because MWCNTs are much thermally stable than SWCNTs, those structure was not drastically changed at similar temperature of SWCNTs but defects in tubes improved at higher than 3000℃ for 30min. These results show that there are worth to further study about chirality change of each wall in MWCNTs and defect healing during heat treatment by HR-TEM analyzing.

These two researches specifically demonstrated the effect of heat treatment as a post-treatment method through experimental results. Of course, further studies are needed, we expect that this structure-controllable mechanism will provide an opportunity to much effectively apply the CNTs to various applications.

V. References

(1) Kroto, H. W.; Heath, J. R.; O'Brien, S. C.; Curl, R. F.; Smalley, R. E. C60: Buckminsterfullerene. *Nature* **1985**, *318* (6042), 162–163. https://doi.org/10.1038/318162a0.

(2) Yadav, B. C.; Kumar, R. Structure , Properties and Applications of Fullerenes. *Int. J. Nanotechnol. Appl. ISSN* **2008**, *0973* (1), 15–24.

(3) Geckeler, K. E.; Samal, S. Syntheses and Properties of Macromolecular Fullerenes, a Review. *Polym. Int.* **1999**, *48* (9), 743–757. https://doi.org/10.1002/(sici)1097-0126(199909)48:9<743::aid-pi246>3.3.co;2-w.

(4) Iijima, S. Helical Microtubules of Graphitic Carbon. *Nature* **1991**, *354* (6348), 56–58. https://doi.org/10.1038/354056a0.

(5) Iijima, S.; Ichihashi, T. Single-Shell Carbon Nanotubes of 1-Nm Diameter. *Nature* **1993**, *363* (6430), 603–605. https://doi.org/10.1038/363603a0.

(6) Novoselov, K. S.; Geim, A. K.; Morozov, S. V; Jiang, D.; Zhang, Y.; Dubonos, S. V; Grigorieva, I. V; Firsov, A. A. Electric Field Effect in Atomically Thin Carbon Films. *Science (80-.).* **2004**, *306* (5696), 666 LP – 669. https://doi.org/10.1126/science.1102896.

(7) Choi, W.; Lahiri, I.; Seelaboyina, R.; Kang, Y. S. Synthesis of Graphene and Its Applications: A Review. *Crit. Rev. Solid State Mater. Sci.* **2010**, *35* (1), 52–71. https://doi.org/10.1080/10408430903505036.

(8) Kharisov, B. I.; Kharissova, O. V. Conventional Carbon Allotropes. In *Carbon Allotropes: Metal-Complex Chemistry, Properties and Applications*; Springer International Publishing: Cham, 2019; pp 9–33. https://doi.org/10.1007/978-3-030-03505-1_2.

(9) Scendo, M.; Staszewska-Samson, K. Effect of Temperature on Anti-Corrosive Properties of Diamond-like Carbon Coating on S355 Steel. *Materials (Basel).* **2019**, *12* (10). https://doi.org/10.3390/ma12101659.

(10) Nessim, G. D. Properties, Synthesis, and Growth Mechanisms of Carbon Nanotubes with Special Focus on Thermal Chemical Vapor Deposition. *Nanoscale* **2010**, *2* (8), 1306–1323. https://doi.org/10.1039/b9nr00427k.

(11) Eatemadi, A.; Daraee, H.; Karimkhanloo, H.; Kouhi, M.; Zarghami, N.; Akbarzadeh, A.; Abasi, M.; Hanifehpour, Y.; Joo, S. W. Carbon Nanotubes: Properties, Synthesis, Purification, and Medical Applications. *Nanoscale Res. Lett.* **2014**, *9* (1), 1–13. https://doi.org/10.1186/1556-276X-9-393.

(12) Zhang, F.; Hou, P. X.; Liu, C.; Cheng, H. M. Epitaxial Growth of Single-Wall Carbon Nanotubes. *Carbon N. Y.* **2016**, *102*, 181–197. https://doi.org/10.1016/j.carbon.2016.02.029.

(13) Odom, T. W.; Huang, J. L.; Kim, P.; Lieber, C. M. Structure and Electronic Properties of Carbon Nanotubes. *J. Phys. Chem. B* **2000**, *104* (13), 2794–2809. https://doi.org/10.1021/jp993592k.

(14) Yu, M. F.; Lourie, O.; Dyer, M. J.; Moloni, K.; Kelly, T. F.; Ruoff, R. S. Strength and Breaking Mechanism of Multiwalled Carbon Nanotubes under Tensile Load. *Science (80-.).* **2000**, *287* (5453), 637–640. https://doi.org/10.1126/science.287.5453.637.

(15) Burgans, L. The Atomic Force Microscopic (Afm) Characterization of Nanomaterials. **2009**, No. June.

(16) Han, Z.; Fina, A. Thermal Conductivity of Carbon Nanotubes and Their Polymer Nanocomposites: A Review. *Prog. Polym. Sci.* **2011**, *36* (7), 914–944. https://doi.org/10.1016/j.progpolymsci.2010.11.004.

(17) Pop, E.; Mann, D.; Wang, Q.; Goodson, K.; Dai, H. Thermal Conductance of an Individual Single-Wall Carbon Nanotube above Room Temperature. *Nano Lett.* **2006**, *6* (1), 96–100. https://doi.org/10.1021/nl052145f.

(18) Arora, N.; Sharma, N. N. Arc Discharge Synthesis of Carbon Nanotubes: Comprehensive Review. *Diam. Relat. Mater.* **2014**, *50*, 135–150. https://doi.org/10.1016/j.diamond.2014.10.001.

(19) Ando, Y.; Zhao, X. Synthesis of Carbon Nanotubes by Arc-Discharge Method. *New Diam. Front. Carbon Technol.* **2006**, *16* (3), 123–137.

(20) Shi, Z.; Lian, Y.; Zhou, X.; Gu, Z.; Zhang, Y.; Iijima, S.; Zhou, L.; Yue, K. T.; Zhang, S. Mass-Production of Single-Wall Carbon Nanotubes by Arc Discharge Method. *Carbon N. Y.* **1999**, *37* (9), 1449–1453. https://doi.org/10.1016/S0008-6223(99)00007-X.

(21) Guo, T.; Nikolaev, P.; Thess, A.; Colbert, D. T.; Smalley, R. E. Catalytic Growth of Single-Walled Manotubes by Laser Vaporization. *Chem. Phys. Lett.* **1995**, *243* (1), 49–54. https://doi.org/https://doi.org/10.1016/0009-2614(95)00825-O.

(22) Scott, C. D.; Arepalli, S.; Nikolaev, P.; Smalley, R. E. Growth Mechanisms for Single-Wall Carbon Nanotubes in a Laser-Ablation Process. *Appl. Phys. A Mater. Sci. Process.* **2001**, *72* (5), 573–580. https://doi.org/10.1007/s003390100761.

(23) Journet, C.; Picher, M.; Jourdain, V. Carbon Nanotube Synthesis: From Large-Scale Production to Atom-by-Atom Growth. *Nanotechnology* **2012**, *23* (14).

https://doi.org/10.1088/0957-4484/23/14/142001.

(24) Thess, A.; Lee, R.; Nikolaev, P.; Dai, H.; Petit, P.; Robert, J.; Xu, C.; Lee, Y. H.; Kim, S. G.; Rinzler, A. G.; Colbert, D. T.; Scuseria, G. E.; Tománek, D.; Fischer, J. E.; Smalley, R. E. Crystalline Ropes of Metallic Carbon Nanotubes. *Science (80-.).* **1996**, *273* (5274), 483–487. https://doi.org/10.1126/science.273.5274.483.

(25) Hata, K.; Futaba, D. N.; Mizuno, K.; Namai, T.; Yumura, M.; Iijima, S. Water-Assisted Highly Efficient Synthesis of Impurity-Free Single-Walled Carbon Nanotubes. *Science (80-.).* **2004**, *306* (5700), 1362–1364. https://doi.org/10.1126/science.1104962.

(26) Maruyama, S.; Einarsson, E.; Murakami, Y.; Edamura, T. Growth Process of Vertically Aligned Single-Walled Carbon Nanotubes. *Chem. Phys. Lett.* **2005**, *403* (4–6), 320–323. https://doi.org/10.1016/j.cplett.2005.01.031.

(27) Ago, H.; Imamura, S.; Okazaki, T.; Saito, T.; Yumura, M.; Tsuji, M. CVD Growth of Single-Walled Carbon Nanotubes with Narrow Diameter Distribution over Fe/MgO Catalyst and Their Fluorescence Spectroscopy. *J. Phys. Chem. B* **2005**, *109* (20), 10035–10041. https://doi.org/10.1021/jp050307q.

(28) Bronikowski, M. J.; Willis, P. A.; Colbert, D. T.; Smith, K. A.; Smalley, R. E. Gas-Phase Production of Carbon Single-Walled Nanotubes from Carbon Monoxide via the HiPco Process: A Parametric Study. *J. Vac. Sci. Technol. A Vacuum, Surfaces, Film.* **2001**, *19* (4), 1800–1805. https://doi.org/10.1116/1.1380721.

(29) Nikolaev, P.; Bronikowski, M. J.; Bradley, R. K.; Rohmund, F.; Colbert, D. T.; Smith, K. A.; Smalley, R. E. Gas-Phase Catalytic Growth of Single-Walled Carbon Nanotubes from Carbon Monoxide. *Chem. Phys. Lett.* **1999**, *313* (1–2), 91–97. https://doi.org/10.1016/S0009-2614(99)01029-5.

(30) Guo, T.; Nikolaev, P.; Thess, A.; Colbert, D. T.; Smalley, R. E. Catalytic Growth of Single-Walled Manotubes by Laser Vaporization. *Chem. Phys. Lett.* **1995**, *243* (1), 49–54. https://doi.org/https://doi.org/10.1016/0009-2614(95)00825-O.

(31) Purohit, R.; Purohit, K.; Rana, S.; Rana, R. S.; Patel, V. Carbon Nanotubes and Their Growth Methods. *Procedia Mater. Sci.* **2014**, *6* (Icmpc), 716–728. https://doi.org/10.1016/j.mspro.2014.07.088.

(32) Maruyama, T. Current Status of Single-Walled Carbon Nanotube Synthesis from Metal Catalysts by Chemical Vapor Deposition. *Mater. Express* **2018**, *8* (1). https://doi.org/10.1166/mex.2018.1407.

(33) Jang, S.; Jang, H.; Lee, Y.; Suh, D.; Baik, S.; Hee Hong, B.; Ahn, J. H. Flexible, Transparent Single-Walled Carbon Nanotube Transistors with Grapheme Electrodes. *Nanotechnology* **2010**, *21* (42). https://doi.org/10.1088/0957-4484/21/42/425201.

(34) Cao, Q.; Hur, S. H.; Zhu, Z. T.; Sun, Y.; Wang, C.; Meitl, M. A.; Shim, M.; Rogers, J. A. Highly Bendable, Transparent Thin-Film Transistors That Use Carbon-Nanotube-Based Conductors and Semiconductors with Elastomeric Dielectrics. *Adv. Mater.* **2006**, *18* (3), 304–309. https://doi.org/10.1002/adma.200501740.

(35) He, M.; Croy, R. G.; Essigmann, J. M.; Swager, T. M. Chemiresistive Carbon Nanotube Sensors for N-Nitrosodialkylamines. *ACS Sensors* **2019**, *4* (10), 2819–2824. https://doi.org/10.1021/acssensors.9b01532.

(36) De Volder, M. F. L.; Tawfick, S. H.; Baughman, R. H.; Hart, A. J. Carbon Nanotubes: Present and Future Commercial Applications. *Science (80-.).* **2013**, *339* (6119), 535–539. https://doi.org/10.1126/science.1222453.

(37) Saini, P.; Choudhary, V.; Singh, B. P.; Mathur, R. B.; Dhawan, S. K. Polyaniline–MWCNT Nanocomposites for Microwave Absorption and EMI Shielding. *Mater. Chem. Phys.* **2009**, *113* (2), 919–926. https://doi.org/https://doi.org/10.1016/j.matchemphys.2008.08.065.

(38) Mishra, P.; Jain, R. Electrochemical Deposition of MWCNT-MnO2/PPy Nano-Composite Application for Microbial Fuel Cells. *Int. J. Hydrogen Energy* **2016**, *41* (47), 22394–22405. https://doi.org/10.1016/j.ijhydene.2016.09.020.

(39) Rajaura, R. S.; Srivastava, S.; Sharma, P. K.; Mathur, S.; Shrivastava, R.; Sharma, S. S.; Vijay, Y. K. Structural and Surface Modification of Carbon Nanotubes for Enhanced Hydrogen Storage Density. *Nano-Structures and Nano-Objects* **2018**, *14*, 57–65. https://doi.org/10.1016/j.nanoso.2018.01.005.

(40) Mi, S.; Soo, K.; Chul, Y.; Soo, Y.; Moon, J.; Jae, D.; Suk, K.; Gak, Y.; Chang, S.; Kim, N.; Frauenheim, T.; Hee, Y. Hydrogen Adsorption and Storage in Carbon Nanotubes. *Synth. Met.* **2000**, 209–216.

(41) Hinds, B. J.; Chopra, N.; Rantell, T.; Andrews, R.; Gavalas, V.; Bachas, L. G. Aligned Multiwalled Carbon Nanotube Membranes. *Science (80-.).* **2004**, *303* (5654), 62–65. https://doi.org/10.1126/science.1092048.

(42) Rizzuto, C.; Pugliese, G.; Bahattab, M. A.; Aljlil, S. A.; Drioli, E.; Tocci, E. Multiwalled Carbon Nanotube Membranes for Water Purification. *Sep. Purif. Technol.* **2018**, *193* (August 2017), 378–385. https://doi.org/10.1016/j.seppur.2017.10.025.

(43) Ayre, G. N.; Uchino, T.; Mazumder, B.; Hector, A. L.; Hutchison, J. L.; Smith, D. C.; Ashburn, P.; De Groot, C. H. On the Mechanism of Carbon Nanotube Formation: The Role of the Catalyst. *J. Phys. Condens. Matter* **2011**, *23* (39). https://doi.org/10.1088/0953-8984/23/39/394201.

(44) Liu, B.; Liu, J.; Tu, X.; Zhang, J.; Zheng, M.; Zhou, C. Chirality-Dependent Vapor-Phase Epitaxial Growth and Termination of Single-Wall Carbon Nanotubes. *Nano Lett.* **2013**, *13* (9), 4416–4421. https://doi.org/10.1021/nl402259k.

(45) Liu, J.; Wang, C.; Tu, X.; Liu, B.; Chen, L.; Zheng, M.; Zhou, C. Chirality-Controlled Synthesis of Single-Wall Carbon Nanotubes Using Vapour-Phase Epitaxy. *Nat Commun* **2012**, *3*, 1199. https://doi.org/10.1038/ncomms2205.

(46) Sanchez-Valencia, J. R.; Dienel, T.; Gröning, O.; Shorubalko, I.; Mueller, A.; Jansen, M.; Amsharov, K.; Ruffieux, P.; Fasel, R. Controlled Synthesis of Single-Chirality Carbon Nanotubes. *Nature* **2014**, *512* (1), 61–64. https://doi.org/10.1038/nature13607.

(47) Yang, F.; Wang, X.; Zhang, D.; Yang, J.; Luo, D.; Xu, Z.; Wei, J.; Wang, J.-Q.; Xu, Z.; Peng, F.; Li, X.; Li, R.; Li, Y.; Li, M.; Bai, X.; Ding, F.; Li, Y. Chirality-Specific Growth of Single-Walled Carbon Nanotubes on Solid Alloy Catalysts. *Nature* **2014**, *510* (7506), 522–524. https://doi.org/10.1038/nature13434.

(48) Hu, Y.; Kang, L.; Zhao, Q.; Zhong, H.; Zhang, S.; Yang, L.; Wang, Z.; Lin, J.; Li, Q.; Zhang, Z.; Peng, L.; Liu, Z.; Zhang, J. Growth of High-Density Horizontally Aligned SWNT Arrays Using Trojan Catalysts. *Nat. Commun.* **2015**, *6*, 1–6. https://doi.org/10.1038/ncomms7099.

(49) Nikolaev, P.; Thess, A.; Rinzler, A. G.; Colbert, D. T.; Smalley, R. E. Diameter Doubling of Single-Wall Nanotubes. *Chem. Phys. Lett.* **1997**, *266* (5–6), 422–426. https://doi.org/10.1016/S0009-2614(97)00053-5.

(50) Yudasaka, M.; Kataura, H.; Ichihashi, T.; Qin, L. C.; Kar, S.; Iijima, S. Diameter Enlargement of HiPco Single-Wall Carbon Nanotubes by Heat Treatment. *NANO Lett.* **2001**, *1* (9), 487–489. https://doi.org/10.1021/nl010037x.

(51) Méténier, K.; Bonnamy, S.; Béguin, F.; Journet, C.; Bernier, P.; Lamy de La Chapelle, M.; Chauvet, O.; Lefrant, S. Coalescence of Single-Walled Carbon Nanotubes and Formation of Multi-Walled Carbon Nanotubes under High-Temperature Treatments. *Carbon N. Y.* **2002**, *40* (10), 1765–1773. https://doi.org/https://doi.org/10.1016/S0008-6223(02)00044-1.

(52) Terrones, M.; Terrones, H.; Banhart, F.; Charlier, J. C.; Ajayan, P. M. Coalescence of Single-Walled Carbon Nanotubes. *Science (80-.).* **2000**, *288* (5469), 1226–1229. https://doi.org/10.1126/science.288.5469.1226.

(53) López, M. J.; Rubio, A.; Alonso, J. A.; Lefrant, S.; Méténier, K.; Bonnamy, S. Patching and Tearing Single-Wall Carbon-Nanotube Ropes into Multiwall Carbon Nanotubes. *Phys. Rev. Lett.* **2002**, *89* (25), 255501. https://doi.org/10.1103/PhysRevLett.89.255501.

(54) Endo, M.; Hayashi, T.; Muramatsu, H.; Kim, Y. A.; Terrones, H.; Terrones, M.; Dresselhaus, M. S. Coalescence of Double-Walled Carbon Nanotubes: Formation of Novel Carbon Bicables. *Nano Lett.* **2004**, *4* (8), 1451–1454. https://doi.org/10.1021/nl0492483.

(55) Andrews, R.; Jacques, D.; Qian, D.; Dickey, E. C. Purification and Structural Annealing of Multiwalled Carbon Nanotubes at Graphitization Temperatures. *Carbon N. Y.* **2001**, *39* (11), 1681–1687. https://doi.org/10.1016/S0008-6223(00)00301-8.

(56) Maheshwari, P. H.; Singh, R.; Mathur, R. B. Effect of Heat Treatment on the Structure and Stability of Multiwalled Carbon Nanotubes Produced by Catalytic Chemical Vapor Deposition Technique. *Mater. Chem. Phys.* **2012**, *134* (1), 412–416. https://doi.org/10.1016/j.matchemphys.2012.03.010.

(57) Yang, X.; Han, Z.; Li, Y.; Chen, D.; Zhang, P.; To, A. C. Heat Welding of Non-Orthogonal X-Junction of Single-Walled Carbon Nanotubes. *Phys. E Low-Dimensional Syst. Nanostructures* **2012**, *46*, 30–32. https://doi.org/10.1016/j.physe.2012.08.015.

(58) Jorio, A.; Pimenta, M. A.; Souza Filho, A. G.; Saito, R.; Dresselhaus, G.; Dresselhaus, M. S. Characterizing Carbon Nanotube Samples with Resonance Raman Scattering. *New J. Phys.* **2003**, *5*. https://doi.org/10.1088/1367-2630/5/1/139.

(59) Dresselhaus, M. S.; Dresselhaus, G.; Jorio, A.; Souza Filho, A. G.; Saito, R. Raman Spectroscopy on Isolated Single Wall Carbon Nanotubes. *Carbon N. Y.* **2002**, *40* (12), 2043–2061. https://doi.org/https://doi.org/10.1016/S0008-6223(02)00066-0.

(60) Dresselhaus, M. S.; Dresselhaus, G.; Saito, R.; Jorio, A. Raman Spectroscopy of Carbon Nanotubes. *Phys. Rep.* **2005**, *409* (2), 47–99. https://doi.org/10.1016/j.physrep.2004.10.006.

(61) Pimenta, M. A.; Marucci, A.; Empedocles, S. A.; Bawendi, M. G.; Hanlon, E. B.; Rao, A. M.; Eklund, P. C.; Smalley, R. E.; Dresselhaus, G.; Dresselhaus, M. S. Raman Modes of Metallic Carbon Nanotubes. *Phys. Rev. B* **1998**, *58* (24), R16016--R16019. https://doi.org/10.1103/PhysRevB.58.R16016.

(62) Eskandari, M. J.; Asadabad, M. A.; Tafrishi, R.; Emamalizadeh, M. Transmission Electron Microscopy Characterization of Different Nanotubes. *Inorg. Nano-Metal Chem.* **2017**, *47* (2), 197–201. https://doi.org/10.1080/15533174.2015.1137317.

(63) Zhang, G.; Qi, P.; Wang, X.; Lu, Y.; Li, X.; Tu, R.; Bangsaruntip, S.; Mann, D.; Zhang, L.;

Dai, H. Selective Etching of Metallic Carbon Nanotubes by Gas-Phase Reaction. *Science (80-.).* **2006**, *314* (5801), 974 LP – 977. https://doi.org/10.1126/science.1133781.

(64) Xu, Z.; Li, H.; Fujisawa, K.; Kim, Y. A.; Endo, M.; Ding, F. Multiple Intra-Tube Junctions in the Inner Tube of Peapod-Derived Double Walled Carbon Nanotubes: Theoretical Study and Experimental Evidence. *Nanoscale* **2012**, *4* (1), 130–136. https://doi.org/10.1039/c1nr10889a.

(65) Ding, F.; Yakobson, B. I. Energy-Driven Kinetic Monte Carlo Method and Its Application in Fullerene Coalescence. *J. Phys. Chem. Lett.* **2014**, *5* (17), 2922–2926. https://doi.org/10.1021/jz501324y.

(66) Ding, F.; Xu, Z.; Yakobson, B. I.; Young, R. J.; Kinloch, I. A.; Cui, S.; Deng, L.; Puech, P.; Monthioux, M. Formation Mechanism of Peapod-Derived Double-Walled Carbon Nanotubes. *Phys. Rev. B* **2010**, *82* (4), 41403. https://doi.org/10.1103/PhysRevB.82.041403.

(67) Huang, W.; Wang, Y.; Luo, G.; Wei, F. 99.9% Purity Multi-Walled Carbon Nanotubes By Vacuum High-Temperature Annealing. *Carbon N. Y.* **2003**, *41* (13), 2585–2590. https://doi.org/10.1016/S0008-6223(03)00330-0.

(68) Lee, C. J.; Park, J. Growth Model of Bamboo-Shaped Carbon Nanotubes by Thermal Chemical Vapor Deposition. *Appl. Phys. Lett.* **2000**, *77* (21), 3397–3399. https://doi.org/10.1063/1.1320851.

(69) Ding, F.; Bolton, K.; Rosén, A. Molecular Dynamics Study of Bamboo-like Carbon Nanotube Nucleation. *J. Electron. Mater.* **2006**, *35* (2), 207–210. https://doi.org/10.1007/BF02692437.

(70) Lin, M.; Tan, J. P. Y.; Boothroyd, C.; Loh, K. P.; Tok, E. S.; Foo, Y. L. Dynamical Observation of Bamboo-like Carbon Nanotube Growth. *Nano Lett.* **2007**, *7* (8), 2234–2238. https://doi.org/10.1021/nl070681x.

VI. Acknowledgements

This work is supported by the Institute for Basic Science (IBS-R019-D1) of South Korea, the Outstanding Research Fund (1.170072.01) of Ulsan National Institute of Science and Technology.

First of all, I would like to thank my advisor, Prof. Feng Ding for his positive guidance and encouragement during master's course. His advice and direction gave me insight for experience and inspired me to research. I could learn how to start a research, what is important in study and leadership. I am confident that experience during master's course in Prof. Ding's group has provided a foundation for me to grow into a better Ph.D candidate. I would also like to thank Prof. Zonghoon Lee and Prof. Han Gi Chae who took charge in thesis evaluation as committee members even in busy schedule.

Especially, I am grateful my family for their patience and trust. Their boundless supports gave me the opportunity to achieve my goal and encouraged me to challenge. Without them, I would not have been possible to finish. Finally, I thank to my friends, especially Jeongseok Oh, Siho Lee who the member of Ulsan and high school friends Dong-Eon Kim, Seungwook Lee. They always encouraged me will be well whenever I was having a hard time and consulted me in positive way.

Thanks to the help of many people, I was able to finish master's course smoothly and I make sure to trying to get it back.